Supplementary Information

Subtle structural alterations in G-quadruplex DNA regulate site specificity of fluorescence light-up probes

Rajendra Kumar[1], Karam Chand[1], Sudipta Bhowmik[1,2], Rabindra Nath Das[1], Snehasish Bhattacharjee[2], Mattias Hedenström[1], and Erik Chorell[1]*

[1] Department of chemistry, Umeå University, 90187, Umeå, Sweden
[2] Department of Biophysics, Molecular Biology & Bioinformatics, University of Calcutta, 92, APC Road, Kolkata 700009, India

Table of Contents

Table S1: Sequences of the DNAs used in the study. In G-Quadruplex DNA, Guanines involved in the G-tetrad formation are highlighted in blue.

DNA				1	2	3	4	5	6	7	8	9	10	11	12	13	14	15	16	17	18	19	20	21	22	23	24	25	26
c-MYC				G	G	A	G	G	G	T	G	G	G	G	A	G	G	G	T	G	G	G	G	A	A	G	G		
Pu24T				T	G	A	G	G	G	T	G	G	T	G	A	G	G	G	T	G	G	G	G	A	A	G	G		
Pu27	T	G	G	G	G	A	G	G	G	T	G	G	G	G	A	G	G	G	T	G	G	G	G	A	A	G	G		
5'ΔTGA-Pu24T							G	G	G	T	G	G	T	G	A	G	G	G	T	G	G	G	G	A	A	G	G		
Pu22				T	G	A	G	G	G	T	G	G	G	T	A	G	G	G	T	G	G	G	T	A	A				
5'ΔTGA-Pu22							G	G	G	T	G	G	G	T	A	G	G	G	T	G	G	G	T	A	A				
3'ΔTAA-Pu22				T	G	A	G	G	G	T	G	G	G	T	A	G	G	G	T	G	G	G							
human telomeric G4 DNA (H-*telo*)				A	G	G	G	T	T	A	G	G	G	T	T	A	G	G	G	T	T	A	G	G	G				
Duplex				C	A	A	T	C	G	G	A	T	C	G	A	A	T	T	C	G	A	T	C	C	G	A	T	T	G

Table S2: Summary of molecular dynamics simulations performed in this study. A total of ~5000 ns MD simulations were performed and further used for the analysis.

G-Quadruplexes	Compound	Binding position	Conformations	Copy	Length (ns)	Total (ns)
Pu24T	**4b**	5'-terminal	2	5	~75	750
Pu24T	**4l**	5'-terminal	2	5	~75	750
Pu24T	**6b**	5'-terminal	2	5	~75	750
Pu22	**4l**	3'-terminal	2	5	~75	750
5'ΔTGA-Pu22	**4l**	5'-terminal	1	5	200	1000
3'ΔTAA-Pu22	**4l**	3'-terminal	1	5	200	1000

Table S3: The three largest clusters during MD simulations of compounds bound to the 5'-terminal of the Pu24T *c-MYC* G4 DNA structure. The number shows the percentage of time that the compounds were in the respective cluster during the simulations.

Time (%)	**4b**	**4l**	**6b**
Cluster-1	19	24	37
Cluster-2	15	19	20
Cluster-3	14	13	10

Table S4: Binding energy of compounds bound to 5'-terminal of the Pu24T *c-MYC* G4 DNA structure. The binding energy were calculated from the first 50 frames nearest to the central structure of the cluster by using the MM/PBSA method with a solvent and solute dielectric constant of 80 and 8 respectively. The error was calculated using block averaging method.

Energy (kJ/mol)	**4b**	**4l**	**6b**
Cluster-1	-202 ± 2	-238 ± 14	-310 ± 4
Cluster-2	-135 ± 4	-262 ± 4	-259 ± 1
Cluster-3	-132 ± 3	-225 ± 3	-236 ± 2

Table S5: Partial atomic charge variance of the compounds. The partial atomic charges were calculated using the RESP method as described in methods section. The charge variance on an atomic group is given by $\sigma = {}^{1}/_{n}\,(\sum_{i=1}^{n} c_i^2)$, where n and c_i is number of atoms and partial atomic charge respectively.

Atomic group	**4b**	**4l**	**6b**
Coumarin ± Julolidine	0.205	0.085	0.023
Benzothiazole	0.070	0.064	0.053

Table S6: Contribution of non-polar solvation energy to compound binding. The calculated MM/PBSA binding energy was decomposed over the residues and the non-polar contribution was extracted from it. This value represents the stacking interaction between compounds and the G4 residues. The yellow and green highlighted cells show the interaction of G4 residues with the benzothiazole and coumarin group, respectively.

Energy (kJ/mol)	Cluster	T1	G2	A3	G4	G8	G13	G17
4b	1	-2 ± 1	-25 ± 3	-9 ± 2	-11 ± 1	-18 ± 2	-10 ± 1	-18 ± 1
	2	-7 ± 8	-5 ± 1	-1 ± 1	-2 ± 1	-20 ± 2	-25 ± 2	-0 ± 1
	3	-1 ± 1	-26 ± 4	-7 ± 3	-1 ± 1	-2 ± 1	-20 ± 2	-25 ± 2
4l	1	-2 ± 1	-27 ± 12	-12 ± 2	-9 ± 1	-18 ± 1	-10 ± 1	-30 ± 2
	2	-2 ± 1	-29 ± 5	-11 ± 2	-12 ± 1	-16 ± 1	-10 ± 1	-32 ± 2
	3	-2 ± 1	-25 ± 6	-7 ± 2	-22 ± 1	-12 ± 1	-26 ± 1	-8 ± 1
6b	1	-4 ± 1	-28 ± 12	-19 ± 2	-19 ± 1	-25 ± 2	-19 ± 2	-42 ± 2
	2	-3 ± 1	-17 ± 4	-15 ± 2	-31 ± 2	-37 ± 2	-19 ± 1	-10 ± 1
	3	-3 ± 1	-18 ± 4	-14 ± 2	-29 ± 2	-41 ± 2	-7 ± 1	-5 ± 1

Table S7: Summary of the dissociation constant (K_d) of **4l** obtained from several fitting of ITC data and the fluorescence competitive displacement assay. nd – not done.

Technique	**G4-DNA**	**Fit**	**K_d1 (μM)**	**K_d2 (μM)**	**ΔH1 (Kcal/mol)**	**ΔH2 (Kcal/mol)**	**N1**	**N2**
Isothermal titration calorimetry	Pu22	1	1.23	66.6	3.90	-11	1.03	5.63
		2	3.28	35.5	-14.6	0.24	0.65	10
		3	3.48	19.2	-17.1	1.13	0.71	5.66
		4	1.78	18.7	-9.39	0.29	0.98	7.08
		5	1.62	25.8	-8.81	-0.57	0.74	8.79
		Average	2.28	33.16	-9.20	-1.98	0.82	7.43
	Pu24T	1	23.6	173	-47.70	16.20	1.09	10
		2	37.5	225	-12.30	-10.60	0.99	8.76
		3	56	191	-21.20	-10.30	0.87	7.58
		4	72.9	193	-55	-1.99	0.97	6.88
		5	78.3	188	-78.40	8.68	1.24	8.44
		Average	53.66	194	-42.78	0.39	1.03	8.33
Competitive displacement assay	Pu22	-	1.67	-	-	-	-	-
	Pu24T	-	nd	-	-	-	-	-

Table S8: Binding energy of **4l** bound to the 3'-terminal of Pu22 *c-MYC* G4 DNA structure. The binding energy was calculated from the first 50 frames nearest to the central structure of the cluster by using the *g_mmpbsa* tool with a solvent and solute dielectric constant of 80 and 8 respectively. The error was calculated using the block averaging method.

Cluster No.	van der Waals Energy	Electrostatic Energy	Polar Solvation Energy	Non-polar Solvation Energy	Binding Energy	Occurrence
1	-165 ± 1	0 ± 1	24 ± 1	-12 ± 1	-153 ± 1	51
2	-144 ± 2	-2 ± 1	35 ± 1	-11 ± 1	-122 ± 3	22
3	-227 ± 3	-1 ± 1	10 ± 1	-16 ± 1	-235 ± 3	22
4	-119 ± 2	-3 ± 1	31 ± 4	-11 ± 1	-102 ± 5	5

Table S9: Binding energy of **4l** bound to Pu22 *c-MYC* G4 DNA structure with deleted flanking nucleotides. The binding energy was calculated separately for clusters using the MM/PBSA method. The four components of the binding energy show their respective contribution to the total binding energy.

	Cluster	van der Waals Energy	Electrostatic Energy	Polar solvation energy	Non-polar solvation energy	Binding energy	Occurence (%)
5'-deleted Pu22	1	-156 ± 1	-2 ± 1	58 ± 4	-10 ± 1	-109 ± 4	29.6
	2	-153 ± 1	1 ± 1	27 ± 2	-10 ± 1	-135 ± 2	24.8
	3	-155 ± 1	0 ± 1	35 ± 2	-10 ± 1	-131 ± 2	23.6
	4	-156 ± 1	-2 ± 1	33 ± 2	-10 ± 1	-136 ± 2	22.0
3'-deleted Pu22	1	-154 ± 1	-2 ± 1	21 ± 1	-10 ± 1	-144 ± 1	51.2
	2	-156 ± 2	1 ± 1	23 ± 1	-10 ± 1	-143 ± 2	28.7
	3	-150 ± 1	2 ± 1	22 ± 1	-10 ± 1	-135 ± 2	12.8
	4	-152 ± 1	-2 ± 1	31 ± 1	-10 ± 1	-134 ± 2	7.3

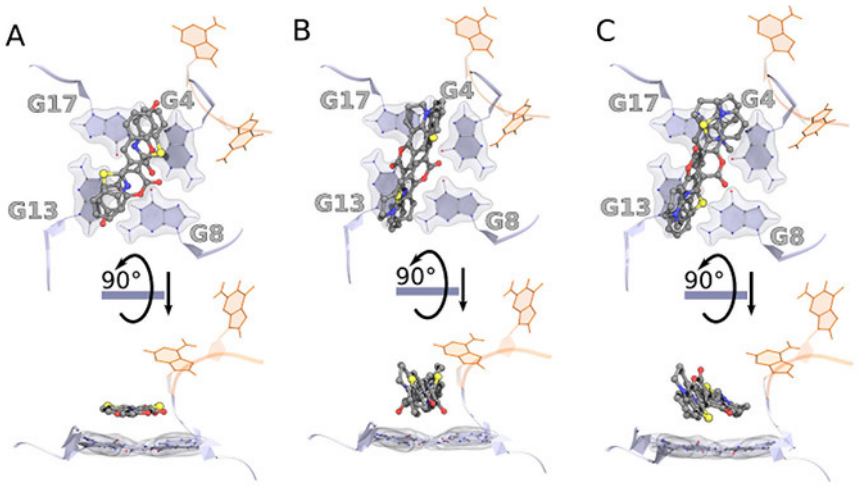

Figure S1: Starting structures for MD simulations. The two binding orientations of (A) **4b** (B) **4l** and (C) **6b** are depicted with respect to the top G-tetrad (*light blue*) and upstream bases (*orange*) that were used as starting conformations for the MD simulations. The two binding orientations were selected such that they are almost opposite to each other.

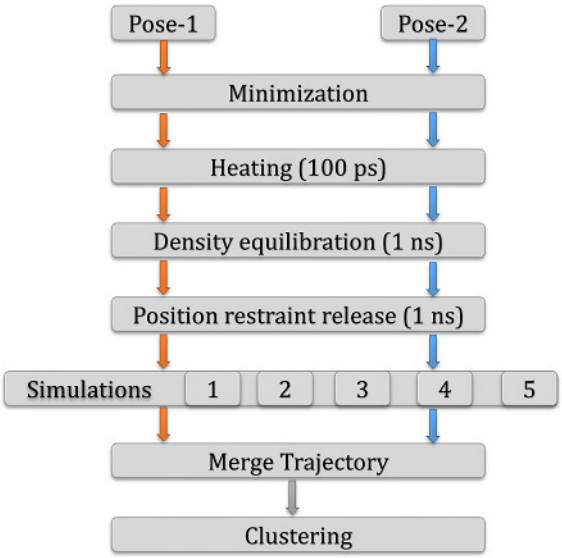

Figure S2: Flow-chart depicting the steps for the MD simulations and the clustering. Two binding modes were considered for each compound and MD simulations were carried out separately for each pose. After production of the simulations, the trajectories from both the binding modes were merged and subjected to subsequent clustering analysis.

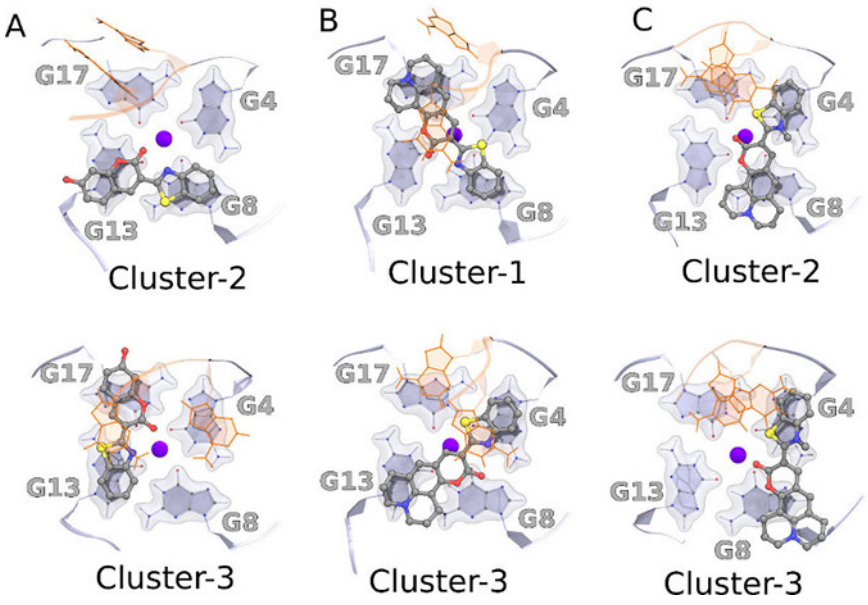

Figure S3: Additional clusters of compounds (A) **4b**, (B) **4l**, and (C) **6b** bound to the 5'-terminal of the Pu24T *c-MYC* G4 DNA structure during MD simulations.

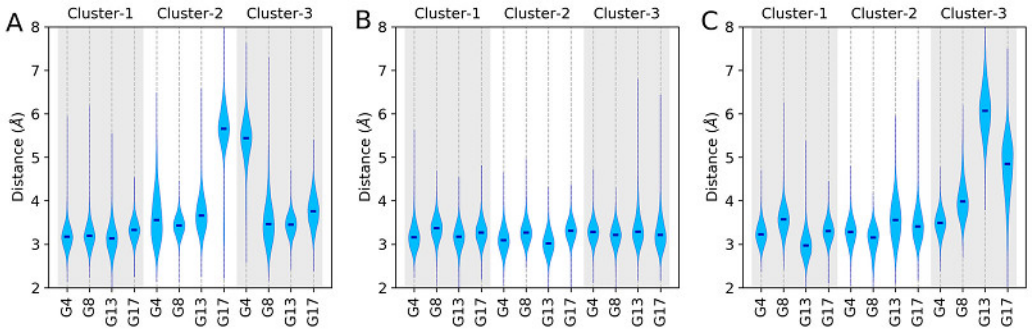

Figure S4: Minimum-distance between the compounds and the Guanine imino-proton in the three largest clusters when the compounds were bound to the 5'-terminal of Pu24T *c-MYC* G4 DNA structure. The distribution of the minimum distance between the Guanine imino-proton and (A) **4b**, (B) **4l**, and (C) **6b** are shown for the three largest clusters. When **4b** binds along the side of the G-tetrad, at least one of the imino-protons (G17 in cluster-2 and G4 in cluster-3) is more than 5 Å away from it.

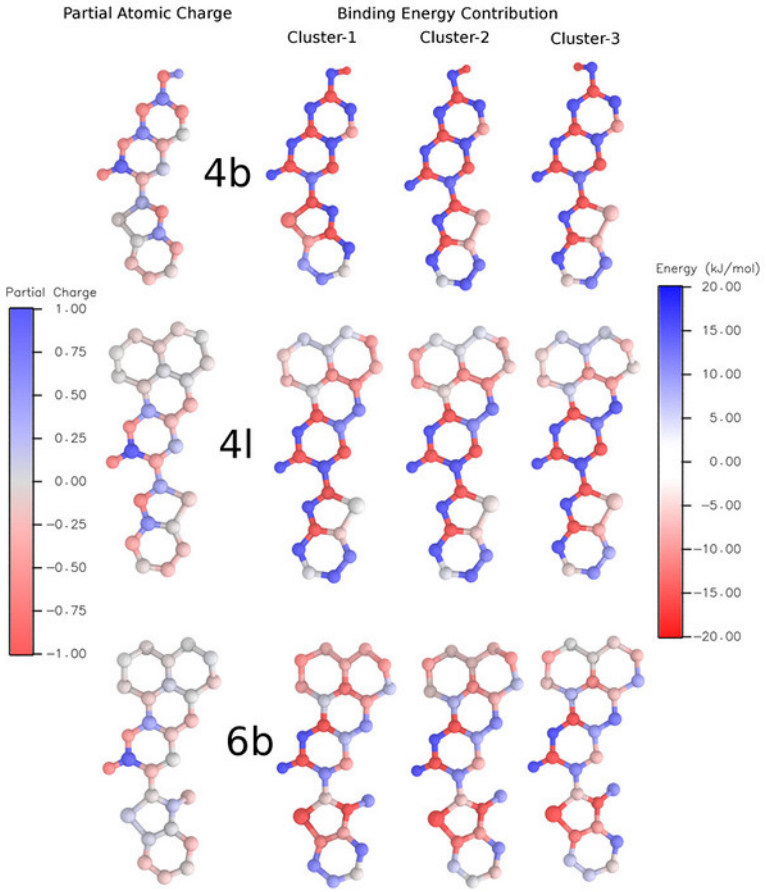

Figure S5: Partial charge distribution and atom-wise binding energy contribution for the compounds when bound to the 5'-terminal of the Pu24T *c-MYC* G4 DNA structure during the MD simulations. To show the relationship between the partial charge distribution and the binding energy contribution, the partial charge distribution (left column) and atom-wise binding energy contribution for the three largest clusters are depicted here (the three columns on the right). Atoms with positive charge (*blue,* columns on the right) have negative binding energy (*red,* column on the left) and vice-versa. The charge variance (the difference between the positive and the negative charge) also affects the binding because a reduction in the negative charge reduces the unfavorable binding contribution of the atom and hence increases the overall binding affinity.

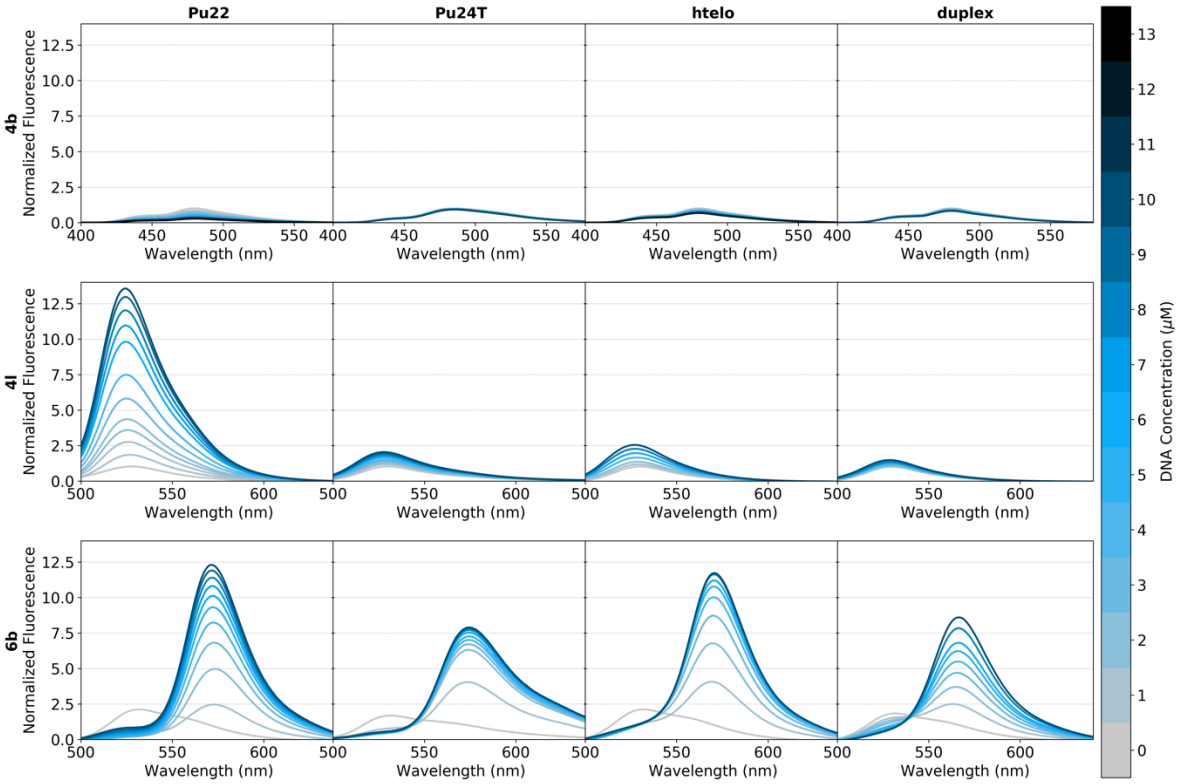

Figure S6: Fluorometric titrations of 5 μM **4b**, **4l** and **6b** with increasing concentrations (0-10μM) of Pu22 *c-MYC* G4 DNA, Pu24T *c-MYC* G4 DNA, human telomeric G4 DNA (H-Telo), and duplex DNA respectively.

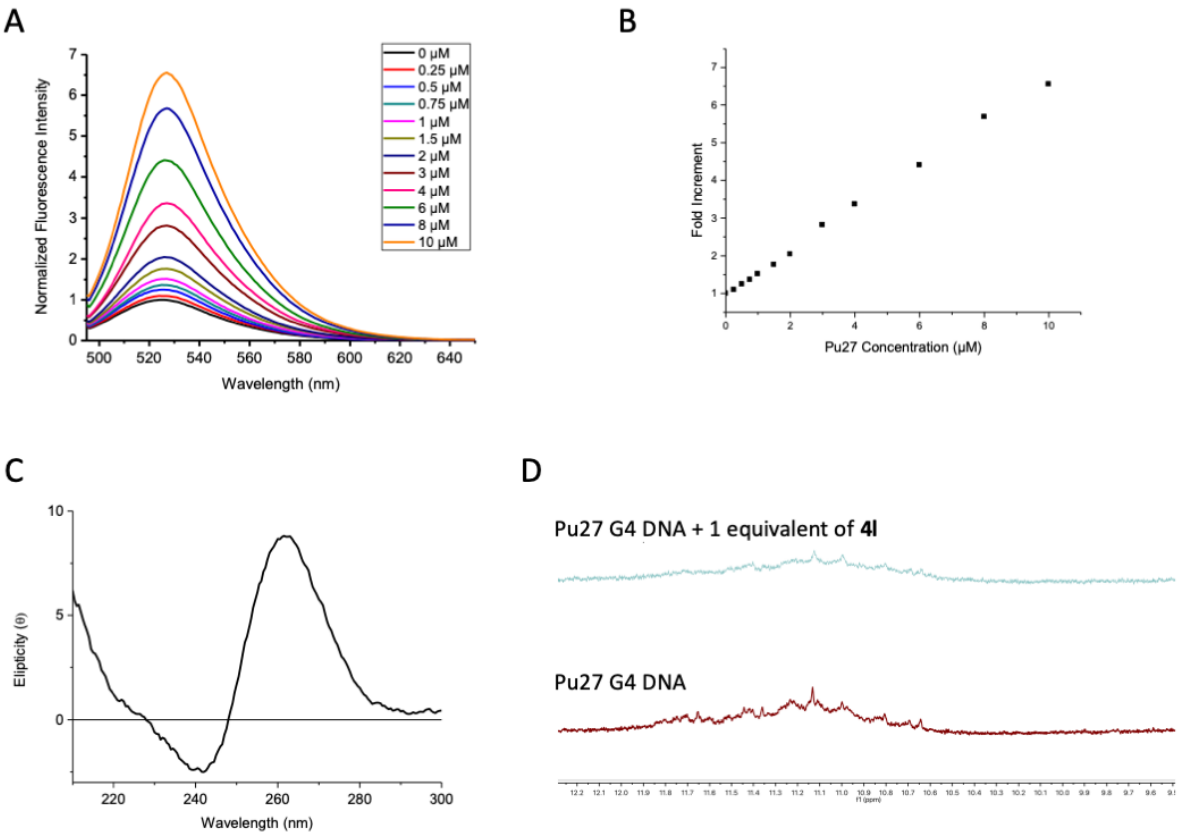

Figure S7. Studies of the pu27 G4 DNA structure. A) and B) Fluorometric titrations of 5 µM **4l** with increasing concentrations (0-10 µM) of Pu27 *c-MYC* G4 DNA showing a 6.5 fold fluorescence increase. C) CD spectrum of Pu27 *c-MYC* G4 DNA showing a parallel topology. D) NMR spectra showing the imino protons of Pu27 *c-MYC* G4 DNA structure alone or after addition of one equivalent of **4l**. Pu27 *c-MYC* G4 DNA is reported to be able to form many different parallel structures wich is the reason for the lack of well-defined peaks. Addition of **4l** clearly affect the spectra suggesting that **4l** is interacting with Pu27 *c-MYC* G4 DNA.

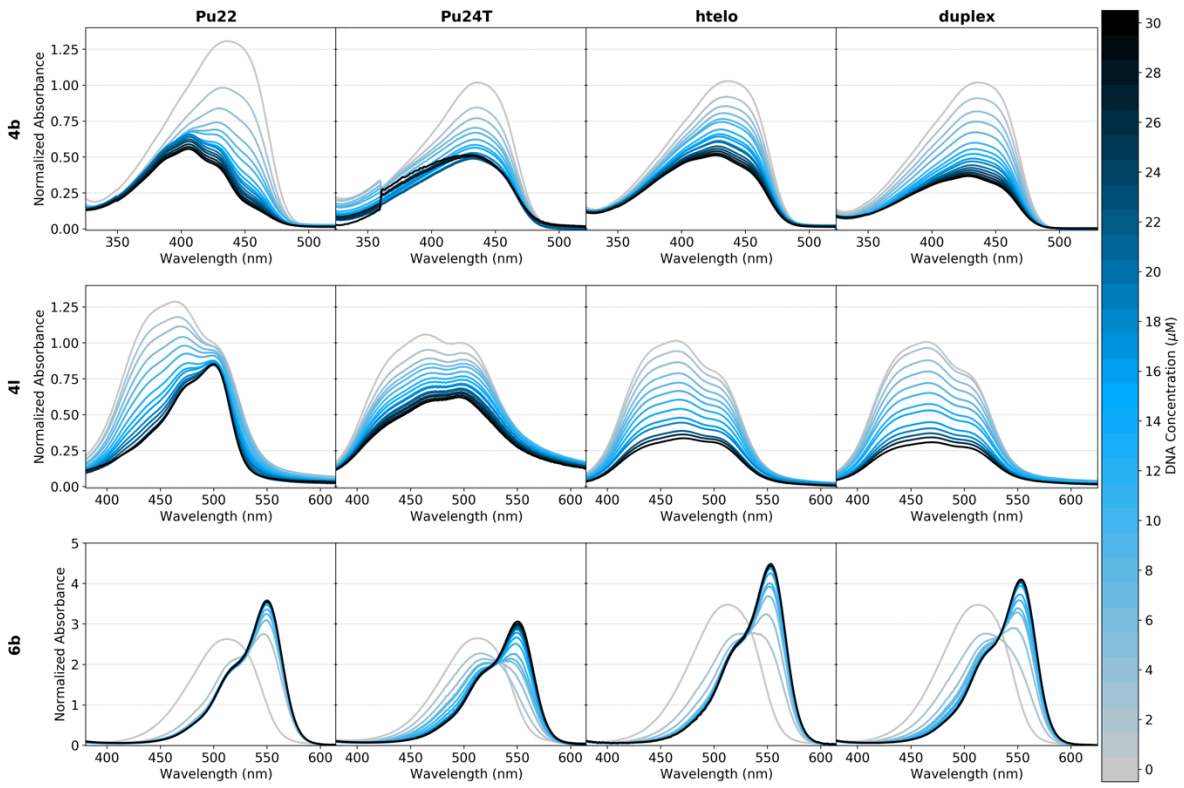

Figure S8: Spectrophotometric titrations of 15 μM **4b**, **4l** and **6b** with increasing concentrations (0-30 μM) of Pu22 *c-MYC* G4 DNA, Pu24T *c-MYC* G4 DNA, human telomeric G4 DNA (H-*Telo*) and duplex DNA.

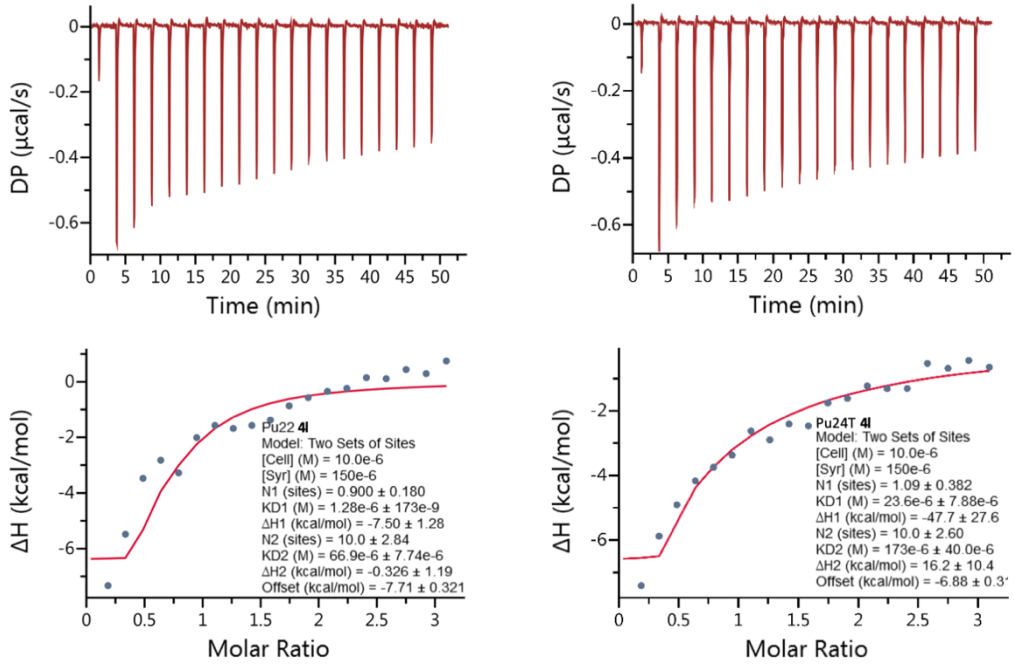

Figure S9. Isothermal Titration Calorimetry (ITC) data (upper Panel) obtained through the addition of Pu22 *c-MYC* G4 DNA or Pu24T *c-MYC* G4 DNA to **4l**. Lower panel shows the corresponding best fit of the data.

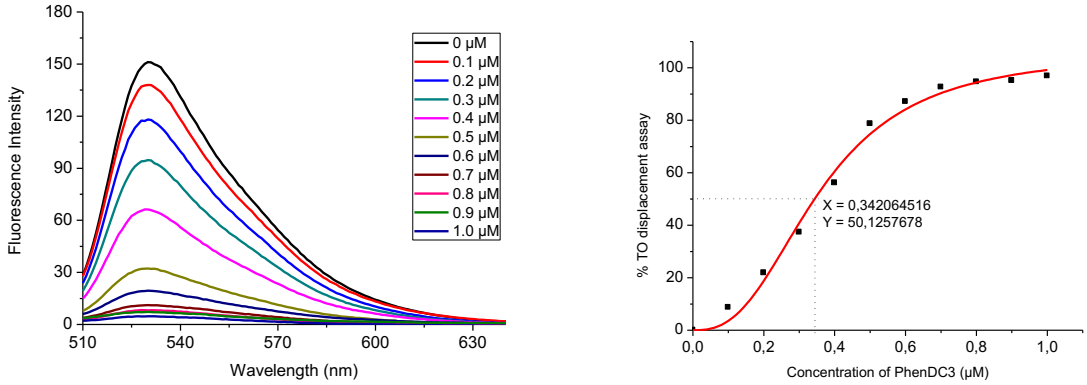

Figure S10. Thiazole Orange (TO) displacement from Pu22 *c-MYC* G4 DNA using Phen-DC3

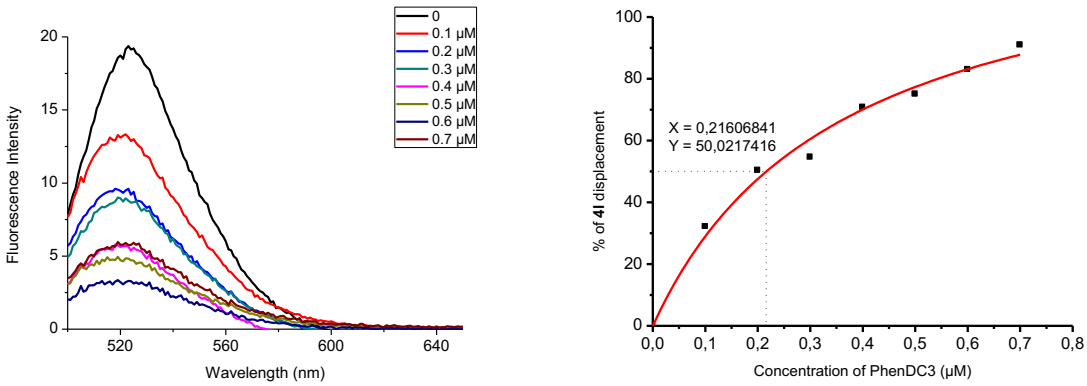

Figure S11. **4l** displacement from Pu22 *c-MYC* G4 DNA using Phen-DC3

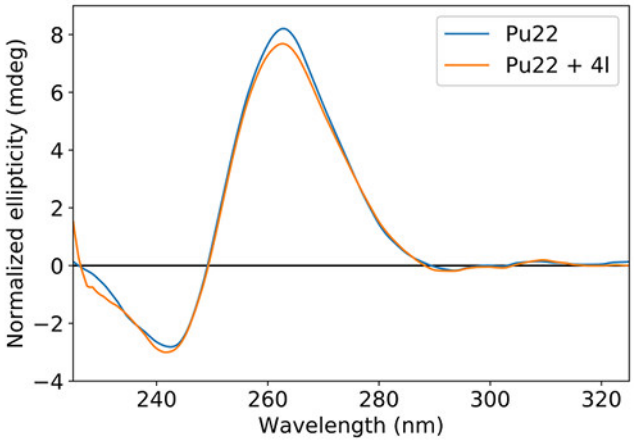

Figure S12: Circular dichroism (CD) spectra of Pu22 *c-MYC* G4 (10 µM) in absence and presence of 8 equivalent of **4l** (80µM).

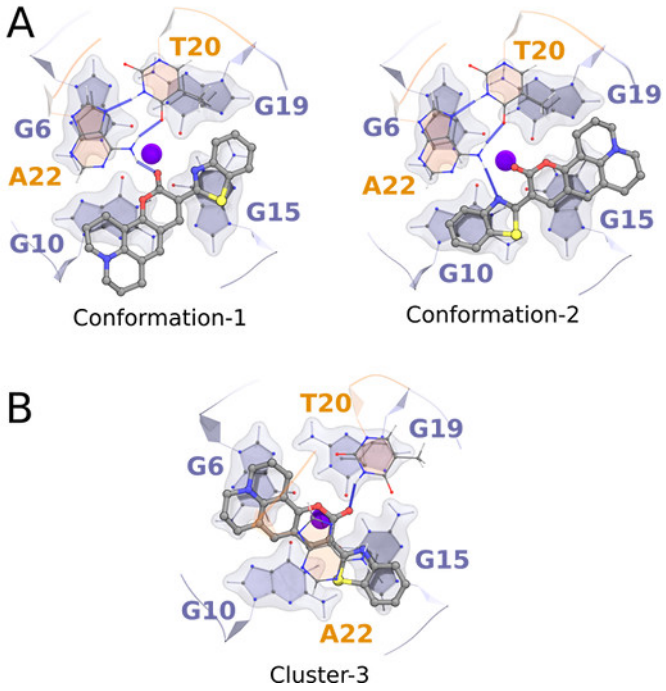

Figure S13: (A) Starting conformations of the **4l**-Pu22 complex. Two conformations of **4l** bound to the Pu22 *c-MYC* G4 DNA structure at the 3'terminal was modeled with hydrogen bonds and used as starting conformation in the MD simulations. (B) The third largest clusters of **4l** bound to the Pu22 *c-MYC* G4 DNA structure at the 3'-terminal. In this cluster, the duplex (T20-A22) broke apart and T20 instead form a hydrogen bond with **4l**.

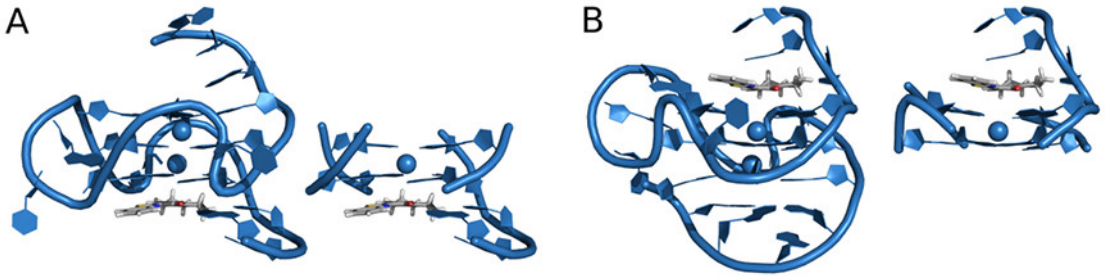

C

3'ΔTAA-Pu22 with **4l**

STATE		ENERGY	EXCITATION	TRANSITION DIPOLE, A.U.			OSCILLATOR
0 ->		HARTREE	EV	X	Y	Z	STRENGTH
0	A	-623.3056274161	0.000				
1	A	-623.2349747922	1.923	0.0972	-0.0131	-0.0537	0.0006
2	A	-623.2319798205	2.004	0.0022	0.0016	0.0016	0.0000
3	A	-623.2306766109	2.040	-0.0139	-0.0029	0.0035	0.0000
4	A	-623.2296975381	2.066	0.0498	-0.0300	0.0059	0.0002
5	A	-623.2289166052	2.087	-0.1829	0.0234	-0.0316	0.0018
6	A	-623.2281587098	2.108	-0.0342	0.0282	-0.0020	0.0001
7	A	-623.2272167385	2.134	-0.5009	0.1242	-0.0506	0.0141
8	A	-623.2262652219	2.160	-0.0695	0.0934	0.0179	0.0007
9	A	-623.2243203028	2.212	0.1892	-0.1698	-0.0239	0.0035
10	A	-623.2236984771	2.229	-0.0189	0.0060	-0.0049	0.0000
11	A	-623.2222001367	2.270	0.0539	-0.0211	-0.0035	0.0002
12	A	-623.2216721343	2.285	-0.0165	0.0070	-0.0010	0.0000
13	**A**	**-623.2190643495**	**2.356**	**2.8899**	**-1.1962**	**0.2057**	**0.5670**
14	A	-623.2177079927	2.392	-0.1895	0.0854	-0.0239	0.0026
15	A	-623.2168525039	2.416	0.2516	-0.1188	0.0512	0.0047
16	A	-623.2146145396	2.477	0.0925	-0.0887	0.0135	0.0010
17	A	-623.2139900397	2.494	-0.0013	0.0002	-0.0002	0.0000
18	A	-623.2103783636	2.592	0.0253	-0.0157	-0.0016	0.0001
19	A	-623.2061626400	2.707	-0.0025	-0.0001	-0.0020	0.0000
20	A	-623.2057287552	2.718	0.0067	-0.0349	-0.0123	0.0001
21	A	-623.2042949671	2.757	0.0038	-0.0019	-0.0027	0.0000
22	A	-623.2031083498	2.790	0.0462	-0.0247	-0.0178	0.0002
23	A	-623.2028954376	2.795	-0.0526	0.0268	0.0091	0.0002
24	A	-623.2014368625	2.835	0.0096	-0.0034	0.0053	0.0000
25	A	-623.2000433330	2.873	-0.0070	0.0032	-0.0018	0.0000
26	A	-623.2000108274	2.874	-0.0015	0.0005	-0.0004	0.0000
27	A	-623.1998885220	2.877	0.0341	-0.0140	0.0064	0.0001
28	A	-623.1992399984	2.895	0.1151	-0.0524	0.0119	0.0011
29	A	-623.1986783621	2.910	-0.0021	0.0009	0.0005	0.0000
30	A	-623.1986579603	2.911	0.0190	-0.0085	0.0017	0.0000

Pu22 with 4l

STATE		ENERGY	EXCITATION	TRANSITION DIPOLE, A.U.			OSCILLATOR
0 ->		HARTREE	EV	X	Y	Z	STRENGTH
0	A	-1233.4579594663	0.000				
1	A	-1233.3883432209	1.894	-0.0458	0.0024	0.0199	0.0001
2	A	-1233.3872908213	1.923	0.0822	-0.0129	-0.0489	0.0004
3	A	-1233.3846743974	1.994	0.0071	0.0015	-0.0084	0.0000
4	A	-1233.3830236231	2.039	-0.0400	0.0029	-0.0127	0.0001
5	A	-1233.3824301814	2.055	-0.2109	0.0293	-0.0328	0.0023
6	A	-1233.3812009950	2.089	0.3919	-0.0735	0.0520	0.0083
7	A	-1233.3807900941	2.100	0.0095	-0.0036	-0.0033	0.0000
8	A	-1233.3799579988	2.123	0.1098	-0.0519	0.0117	0.0008
9	A	-1233.3789130106	2.151	0.0675	-0.0615	-0.0075	0.0004
10	A	-1233.3787898163	2.154	-0.0757	0.0660	0.0048	0.0005
11	A	-1233.3771686786	2.198	0.1814	-0.1499	-0.0127	0.0030
12	A	-1233.3769773458	2.204	0.0868	-0.0917	-0.0125	0.0009
13	A	-1233.3755131196	2.243	0.0026	-0.0056	-0.0002	0.0000
14	A	-1233.3746482789	2.267	-0.0280	0.0223	0.0031	0.0001
15	A	-1233.3741376229	2.281	0.0438	-0.0222	0.0019	0.0001
16	A	-1233.3741262800	2.281	-0.0713	0.0305	-0.0001	0.0003
17	**A**	**-1233.3713867281**	**2.356**	**-2.8673**	**1.1852**	**-0.2413**	**0.5589**
18	A	-1233.3706549171	2.376	0.1150	-0.0488	0.0110	0.0009
19	A	-1233.3692215048	2.415	-0.0000	0.0000	-0.0000	0.0000
20	A	-1233.3685849607	2.432	0.0018	-0.0010	0.0006	0.0000
21	A	-1233.3674083258	2.464	0.1140	-0.0597	0.0434	0.0011
22	A	-1233.3671125911	2.472	-0.0011	0.0006	-0.0001	0.0000
23	A	-1233.3658888071	2.505	-0.0673	0.0771	-0.0152	0.0007
24	A	-1233.3645493242	2.542	-0.0009	0.0001	-0.0002	0.0000
25	A	-1233.3614233594	2.627	-0.0010	0.0013	-0.0009	0.0000
26	A	-1233.3613765186	2.628	-0.0002	0.0022	0.0004	0.0000
27	A	-1233.3602490291	2.659	0.0005	-0.0017	0.0006	0.0000
28	A	-1233.3600684690	2.664	0.0240	-0.0141	-0.0006	0.0001
29	A	-1233.3594024836	2.682	0.0000	-0.0000	-0.0000	0.0000
30	A	-1233.3587322345	2.700	0.0025	-0.0004	-0.0004	0.0000

Figure S14: Truncated structures and spectra of **4l** bound to the Pu24T and Pu22 *c-MYC* G4 DNA. (A) Whole structure of Pu22 (left) with **4l** compared to the truncated structure (right). (B) Whole structure of Pu24T (left) with **4l** compared to the truncated structure (right). (C) Comparison of the GAMESS output for the entire and truncated structure of Pu22-**4l** showing that the largest peak (highlighted by *red*) was obtained at the same excitation energy (2.356 eV). Therefore, truncation does not affect the excitation energy of the largest peak.

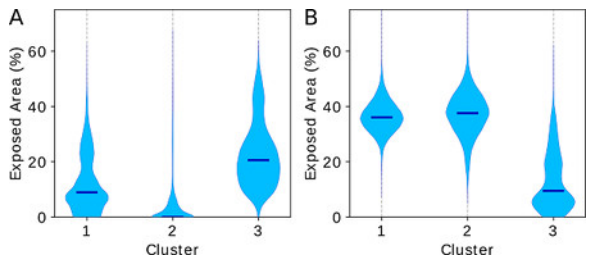

Figure S15: Exposed fraction area of the coumarin ring in **4l** bound to (A) the 5'-terminal of Pu24T *c-MYC* G4 DNA structure and (B) The 3'-terminal of the Pu22 *c-MYC* G4 DNA structure during the MD simulations.

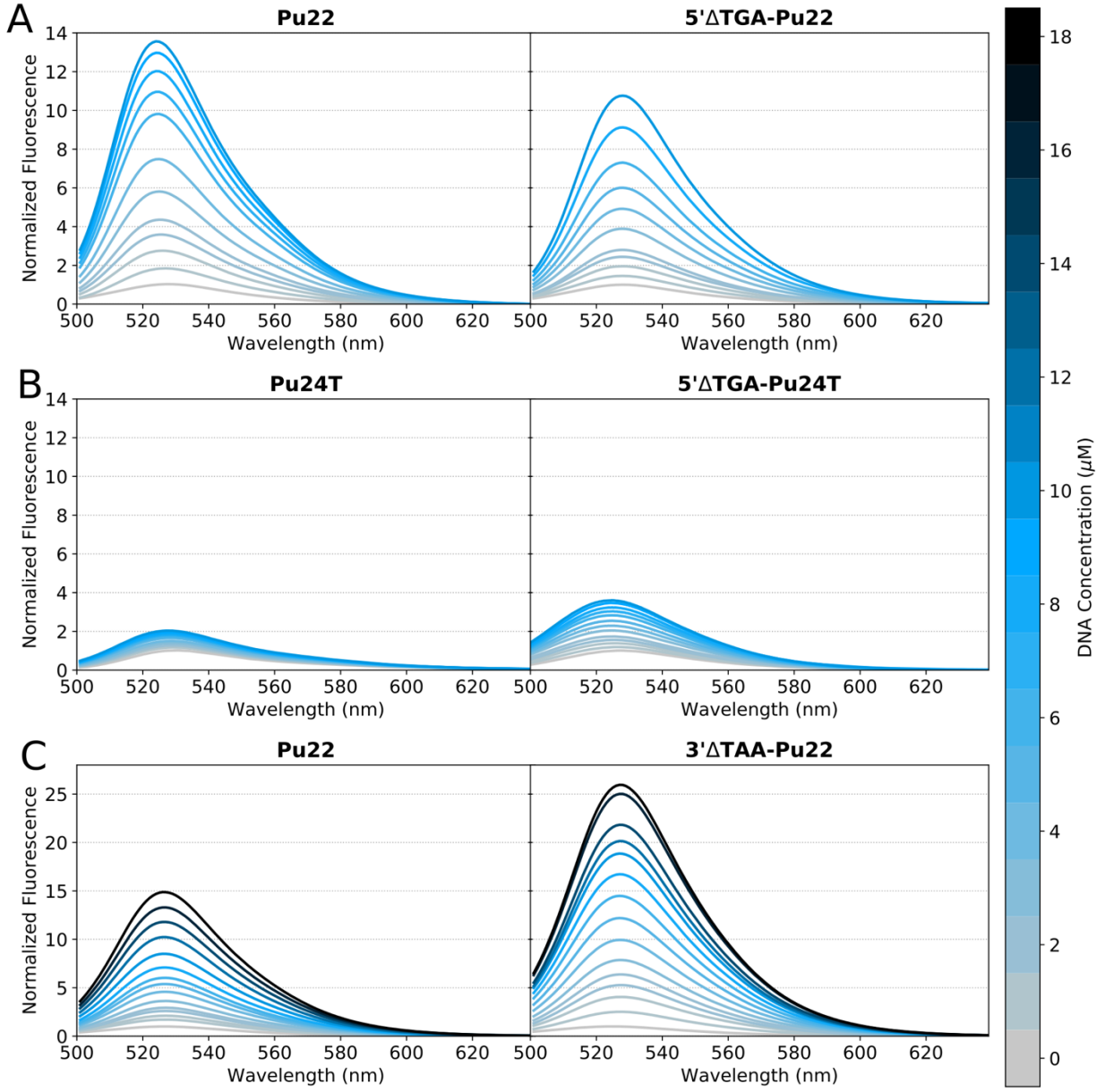

Figure S16: (A, B) Fluorometric titrations of 5 μM of **4l** with increasing concentration of Pu22 *c-MYC* G4, 5'ΔTGA-Pu22 and Pu24T *c-MYC* G4, 5'ΔTGA-Pu24T respectively; (C) Fluorometric titrations of 2.5 μM of **4l** with increasing concentration of Pu22 *c-MYC* G4 and 3'ΔTAA-Pu22.

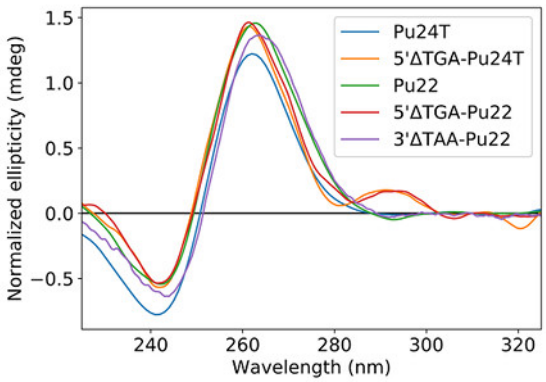

Figure S17: Circular dichroism (CD) spectra of Pu24T *c-MYC* G4, 5'ΔTGA-Pu24T, Pu22 *c-MYC* G4, 5'ΔTGA-Pu22 and 3'ΔTAA-Pu22.

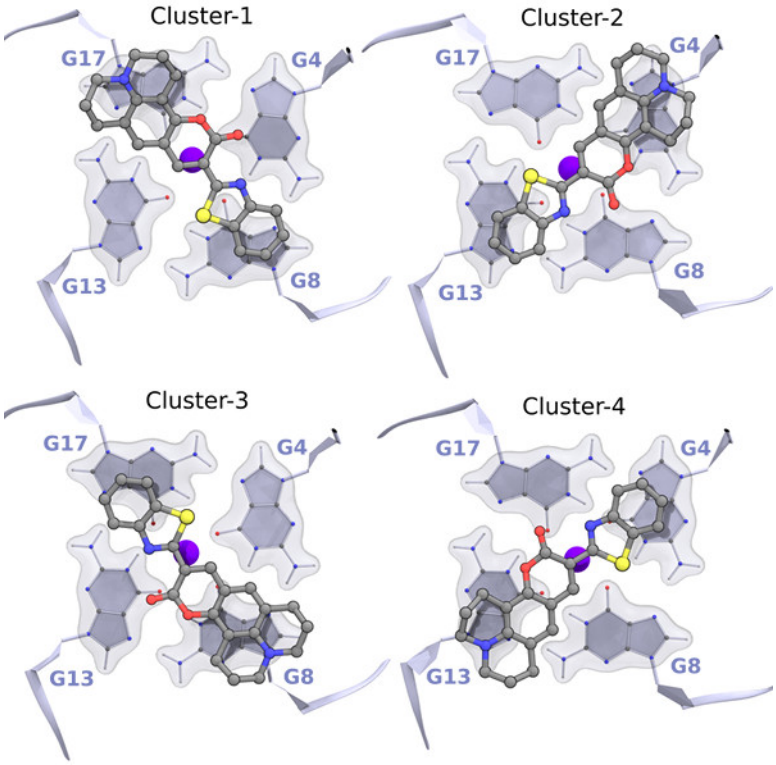

Figure S18: Four binding modes of **4l** in the 5'ΔTGA-Pu22 *c-MYC* G4 DNA structure during the MD simulations.

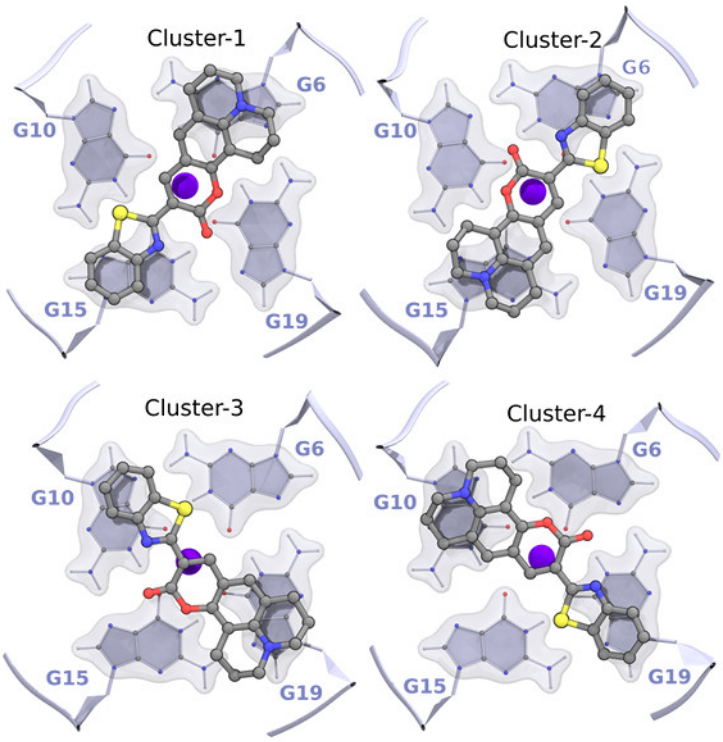

Figure S19: Binding modes of **4l** in the 3'ΔTAA-Pu22 *c-MYC* G4 DNA structure during the MD simulations.

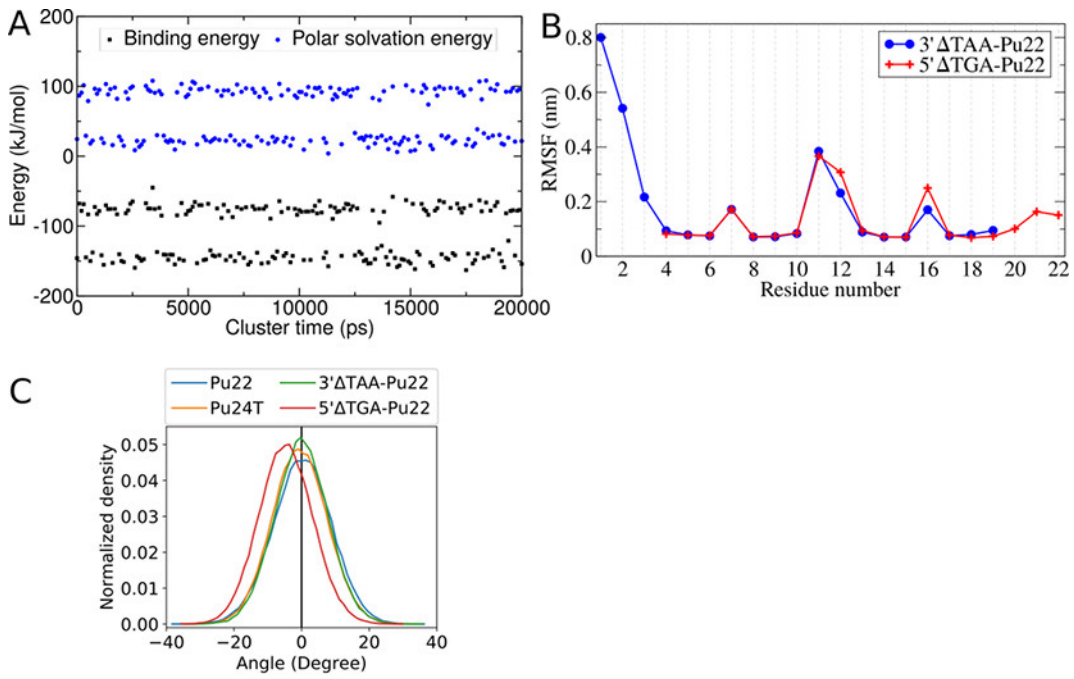

Figure S20: (A) Polar-solvation energy as a function of cluster-time for **4l** bound to the 5'ΔTGA-Pu22 *c-MYC* G4 DNA structure. This energy is calculated for largest cluster. The resulting fluctuation in total binding energy correlates with the polar-solvation energy. (B) Root mean square fluctuations (RMSF) as a function of residues during the simulations. The RMSF was calculated from the combined trajectories and therefore shows the flexibility from the entire simulations. (C) Distribution of planner conformation of 4l during the MD simulations when it is bound to either the 3'terminal Pu22 (*blue*) or the 5'terminal Pu24T (*orange*) or the 3'ΔTAA-Pu22 (*green*) or the 5'ΔTGA-Pu22 (*red*).

Synthesis experimental

All reagents and solvents were used as such received from commercial suppliers unless stated otherwise. TLC was performed on aluminium backed silica gel plates (median pore size 60 Å, fluorescent indicator 254 nm) and detected with UV light. DMF was dried in a solvent drying system (activated molecular sieves in combination with an isocyanate scrubber). Microwave reactions were carried out in an Initiator+ microwave instrument from Biotage, using sealed 0.2–0.5 mL and 10-20 mL process vials. ^{1}H and ^{13}C NMR spectra were recorded on Bruker 400 or 600 MHz spectrometers at 298 K and calibrated by using the residual peak of the solvents as the internal standard (DMSO-d_6: δ H = 2.50 ppm; δ C = 39.50 ppm and $CDCl_3$: δ H = 7.26 ppm; δ C = 77.02 ppm). The abbreviations used in the NMR data are mentioned as singlet = s, doublet = d,triplet = t, multiplet = m, doubledoublet = dd, and broad singlet = brs. LC-MS was conducted on an Agilent 6150 Series Quadrupole LC/MS system. HRMS was performed by using an Agilent 1290 binary LC system connected to an Agilent 6230 Accurate-Mass TOF LC/MS (ESI+); calibrated with an Agilent G1969-85001 ES-TOF Reference Mix containing ammonium trifluoroacetate, purine and hexakis(1*H*,1*H*,3*H*-tetrafluoropropoxy)phosphazine in 90 : 10 acetonitrile : water.

General procedure for the preparation of coumarin-benzothaizole 4(a-m) and coumarin-benzoimidazole (5a-b) derivatives: To the mixture of the respective *ortho*-hydroxyl benzaldehydes **1**(**a**-**m**) (500mg, 4.09 mmol) and 2-benzothaizoleacetonitrile (856 mg, 4.91 mmol) or 2-benzimidazoleacetonitrile (772 mg, 4.91 mmol) in anhydrous ethanol (50 ml) was added with piperidine (81 μL, 0.82 mmol). After addition of piperidine, the reaction mixture become a clear solution within 30 min and the reaction was allowed to stir for 12h. The appearance of precipitates in the reaction mixture indicates the formation of product and progress of reaction was monitored on TLC till consumption of all starting material. The precipitate was filtered and washed with ethanol under reduced pressure to give a yellow to brown colored residue of iminocoumarin derivatives (**2a**-**m** & **3a**-**b**). The residue so obtained was then taken in 2M hydrochloric acid (50 mL) and the suspension was heated to reflux until complete hydrolysis of the iminocoumarin (as monitored by TLC or LC-MS)**.** The suspension was then filtered and washed with saturated bicarbonate solution followed by water. The crystallization of the filtrated

residue in ethanol gave the desired coumarin-benzothaizole **4**(**a**-**m**) and coumarin-benzoimidazole (**5a**-**b**) derivatives in pure form with quantitative yield.

(4a) **3-(Benzo[d]thiazol-2-yl)-7-(diethylamino)-2H-chromen-2-one** (ECH-106): The title compound (**4a**) was obtained from the reaction of 4-(diethylamino)-2-hydroxybenzaldehyde (**1a**) with 2-benzothaizoleacetonitrile as a yellow solid in 63% yield by following the general procedure. ^{1}H NMR (400MHz, $CDCl_3$) δ (ppm): 8.92 (s, 1H), 8.02 (d, *J* = 8.0Hz, 1H), 7.95 (d, *J* = 8.0Hz, 1H), 7.47-7.51 (m, 2H), 7.37 (t, *J* = 8.0 Hz, 1H), 3.47 (q, *J* = 8.0 Hz, 4H), 1.26 (t, *J* = 8.0 Hz, 6H); ^{13}C NMR (100MHz, DMSO-d_6) δ (ppm): 161.82, 161.09, 157.06, 152.58, 152.09, 142.04, 136.28, 130.79, 126.09, 124.44, 122.12, 121.61, 112.49, 109.96, 108.69, 97.00, 45.11, 12.50; m/z (ESI MS): calculated $C_{20}H_{19}N_2O_2S$ $(M+H)^+$: 351.116; obtained 351.2.

(4b) **3-(Benzo[d]thiazol-2-yl)-7-hydroxy-2H-chromen-2-one** (ECH-107): The title compound (**4b**) was obtained from the reaction of 2,4-dihydroxybenzaldehyde (**1b**) with 2-benzothaizoleacetonitrile as a yellow solid in 76% yield by following the general procedure. ^{1}H-NMR (400MHz, DMSO-d_6) δ (ppm): 8.87 (s, 1H), 8.07 (d, *J* = 8.0 Hz, 1H), 7.94 (d, *J* = 8.0 Hz, 1H), 7.60 (d, *J* = 8.0 Hz, 1H), 7.49 (t, *J* = 8.0 Hz, 1H), 7.36 (t, *J* = 8.0 Hz, 1H), 6.50 (dd, *J* = 4.0 & 8.0Hz), 6.32 (s, 1Hz); ^{13}C NMR (100MHz, DMSO-d_6) δ (ppm): 161.40, 161.03, 158.16, 152.74, 142.29, 135.63, 132.08, 126.56, 124.45, 122.27, 121.84, 119.21, 108.66, 103.16; m/z (HRMS): calculated for $C_{16}H_{10}NO_3S$ $(M+H)^+$: 296.0376; obtained 296.0381. HPLC purity 100%.

(4c) **3-(Benzo[d]thiazol-2-yl)-7-methoxy-2H-chromen-2-one** (ECH-108): The title compound (**4c**) was obtained from the reaction of 2-hydroxy-4-methoxybenzaldehyde (**1c**) with 2-benzothaizoleacetonitrile as a yellow solid in 69% yield by following the general procedure. ^{1}H NMR (400MHz, $CDCl_3$) δ (ppm): 9.03 (s, 1H), 8.07 (d, *J* = 8.0 Hz, 1H), 7.97 (d, *J* = 8.0 Hz, 1H), 7.63 (d, *J* = 8.0 Hz, 1H), 7.52 (t, *J* = 8.0 Hz, 1H), 7.41 (t, *J* = 8.0 Hz, 1H), 7.41 (t, *J* = 8.0 Hz, 1H), 6.96 (dd, *J* = 4.0 & 8.0 Hz, 1H), 6.92 (d, *J* = 8.0 Hz, 1H), 3.93 (s, 3H); ^{13}C NMR (100MHz, DMSO-d_6) δ (ppm): 164.28, 160.48, 160.24, 156.04, 152.48, 141.73, 136.60, 130.50, 126.37, 125.09, 122.64, 121.73, 116.84, 113.97, 112.74, 100.57, 56.02; m/z (ESI MS): calculated for $C_{17}H_{12}NO_3S$ $(M+H)^+$: 310.05; obtained 310.2.

(4d) **3-(Benzo[d]thiazol-2-yl)-2H-chromen-2-one** (ECH-109): The title compound (**4d**) was obtained from the reaction of 2-hydroxybenzaldehyde (**1d**) with 2-benzothaizoleacetonitrile as a yellow solid in 71% yield by following the general procedure. ^{1}H NMR (400MHz, $CDCl_3$) δ (ppm): 9.09 (s, 1H), 8.10 (d, *J* = 8.0 Hz, 1H), 8.00 (d, *J* = 8.0 Hz, 1H), 7.74 (d, *J* = 8.0 Hz, 1H), 7.65 (t, *J* = 8.0 Hz, 1H), 7.55 (t, *J* = 8.0 Hz, 1H), 7.44-7.47 (m, 2H), 7.38-7.41 (m, 2H); ^{13}C NMR (100MHz, DMSO-d_6) δ (ppm): 159.89, 153.87, 152.45, 141.49, 136.84, 133.24, 129.39, 126.53, 125.44, 125.24, 122.93, 121.80, 120.37, 119.01, 116.81; m/z (ESI MS): calculated for $C_{16}H_{10}NO_2S$ $(M+H)^+$: 280.043; obtained 280.1.

(4e) **3-(Benzo[d]thiazol-2-yl)-8-methoxy-2H-chromen-2-one** (ECH-110): The title compound (**4e**) was obtained from the reaction of 2-hydroxy-3-methoxybenzaldehyde (**1e**) with 2-benzothaizoleacetonitrile as a yellow solid in 74% yield by following the general procedure. ^{1}H NMR (400MHz, $CDCl_3$) δ (ppm): 9.06 (s, 1H), 8.09 (d, *J* = 8.0 Hz, 1H), 7.99 (d, *J* = 8.0 Hz, 1H), 7.54 (t, *J* = 8.0 Hz, 1H), 7.43 (t, *J* = 8.0 Hz, 1H), 7.31-7.32 (m, 2H), 7.219 (dd, *J* = 4.0 & 8.0 Hz, 1H), 7.13 (d, , *J* = 4.0 Hz, 2H), 3.89 (s, 3H); ^{13}C NMR (100MHz, $CDCl_3$) δ (ppm): 159.87, 159.38, 152.47, 147.21, 143.53, 141.63, 136.89, 126.49, 125.40, 125.07, 122.91, 121.79, 120.65, 120.56, 119.64, 114.93, 56.40; m/z (ESI MS): calculated for $C_{17}H_{12}NO_3S$ $(M+H)^+$: 310.05; obtained 310.2.

(4f) **3-(Benzo[d]thiazol-2-yl)-8-hydroxy-2H-chromen-2-one** (ECH-111): The title compound (**4f**) was obtained from the reaction of 2,3-dihydroxybenzaldehyde (**1f**) with 2-benzothaizoleacetonitrile as a yellow solid in 71% yield by following the general procedure. ^{1}H NMR (400MHz, DMSO-d_6) δ (ppm): 10.47 (brs, 1H), 9.21 (s, 1H), 8.21 (d, *J* = 8.0 Hz, 1H), 8.10 (d, *J* = 8.0 Hz, 1H), 7.60 (t, *J* = 8.0 Hz, 1H), 7.48-7.52 (m, *2*H), 7.24-7.30 (m, 2H); ^{13}C NMR (100MHz, DMSO-d_6) δ (ppm): 160.31, 159.81, 152.41, 145.04, 142.98, 142.51, 136.42, 127.17, 125.92, 125.68, 123.01, 122.74, 120.67, 120.38, 120.25, 119.71; m/z (ESI MS): calculated for $C_{16}H_{10}NO_3S$ $(M+H)^+$: 296.04; obtained 296.2.

(4g) **3-(Benzo[d]thiazol-2-yl)-8-nitro-2H-chromen-2-one** (ECH-112): The title compound (**4g**) was obtained from the reaction of 2,3-dihydroxybenzaldehyde (**1g**) with 2-benzothaizoleacetonitrile as a yellow solid in 74% yield by following the general procedure. ^{1}H NMR (600 MHz, DMSO-d_6) δ (ppm): 9.36 (s, 1H), 8.45 (d, *J* = 8.0 Hz, 1H), 8.40 (d, *J* = 8.0 Hz, 1H), 8.23(d, *J* = 8.0 Hz, 1H), 8.13 (d, *J* = 8.0 Hz, 1H), 7.60-7.66 (m, 2H), 7.53 (t, *J* = 8.0 Hz, 1H); ^{13}C NMR (150 MHz, DMSO-

d$_6$) δ (ppm): 159.51, 158.35, 152.41, 145.96, 141.43, 137.07, 136.51, 136.00, 128.93, 127.39, 126.27, 125.23, 123.20, 122.90, 121.42, 121.26, m/z (ESI MS): not ionised.

(4h) **3-(benzo[d]thiazol-2-yl)-6-methoxy-2H-chromen-2-one** (ECH-113): The title compound (**4h**) was obtained from the reaction of 2-hydroxy-5-methoxybenzaldehyde (**1h**) with 2-benzothaizoleacetonitrile as a yellow solid in 71% yield by following the general procedure. ^{1}H NMR (400MHz, $CDCl_3$) δ (ppm): 9.04 (s, 1H), 8.08 (d, *J* = 8.0 Hz, 1H), 7.98 (d, *J* = 8.0 Hz, 1H), 7.53 (t, *J* = 8.0 Hz, 1H), 7.43 (t, *J* = 8.0 Hz, 1H), 7.37 (d, *J* = 8.0 Hz, 1H), 7.22 (dd, *J* = 4.0 & 8.0 Hz, 1H), 7.13 (d, , *J* = 4.0 Hz, 2H), 3.89 (s, 3H); ^{13}C NMR (100MHz, $CDCl_3$) δ (ppm): 160.02, 159.91, 156.57, 152.46, 148.45, 141.28, 136.89, 126.49, 125.40, 122.91, 121.79, 121.48, 120.54, 119.34, 117.85, 110.61, 55.90; m/z (ESI MS): calculated for $C_{17}H_{12}NO_3S$ $(M+H)^+$: 310.05; obtained 310.2.

(4i) **3-(benzo[d]thiazol-2-yl)-6-hydroxy-2H-chromen-2-one** (ECH-114): The title compound (**4i**) was obtained from the reaction of 2,5-dihydroxybenzaldehyde (**1i**) with 2-benzothaizoleacetonitrile as a yellow solid in 70% yield by following the general procedure. ^{1}H NMR (400MHz, DMSO-*d*$_6$) δ (ppm): 9.25 (s, 1H), 8.26 (d, *J* = 8.0 Hz, 1H), 8.16 (d, *J* = 8.0 Hz, 1H), 7.66 (t, *J* = 8.0 Hz, 1H), 7.56 (t, *J* = 8.0 Hz, 1H), 7.44-7.48 (m, 2H), 7.25 (dd, *J* = 4.0 & 8.0 Hz); ^{13}C NMR (100MHz, DMSO-*d*$_6$) δ (ppm): 160.40, 160.09, 154.80, 152.40, 147.36, 142.56, 136.45, 127.17, 125.90, 122.99, 122.74, 122.51, 119.86, 119.75, 117.67, 114.30, m/z (ESI MS): calculated for $C_{16}H_{10}NO_3S$ $(M+H)^+$: 296.04; obtained 296.1.

(4j) **3-(Benzo[d]thiazol-2-yl)-6-fluoro-2H-chromen-2-one** (ECH-115): The title compound (**4j**) was obtained from the reaction of 5-fluoro-2-hydroxybenzaldehyde (**1j**) with 2-benzothaizoleacetonitrile as a yellow solid in 67% yield by following the general procedure. ^{1}H NMR (400MHz, $CDCl_3$) δ (ppm): 9.02 (s, 1H), 8.10 (d, *J* = 8.0 Hz, 1H), 7.99 (d, *J* = 8.0 Hz, 1H), 7.55 (t, *J* = 8.0 Hz, 1H), 7.34-7.47 (m, 4H); ^{13}C NMR (100MHz, $CDCl_3$) δ (ppm): 160.33, 159.50 ($J_{C\text{-}F}$ = 96.0Hz), 157.88, 152.44, 150.00 ($J_{C\text{-}F}$ = 8.0Hz), 140.27 ($J_{C\text{-}F}$ = 12.0Hz), 136.96, 126.64, 125.65, 123.08, 121.82, 121.40, 120.72 ($J_{C\text{-}F}$ = 100.0Hz), 119.69 ($J_{C\text{-}F}$ = 36.0Hz), 118.43 ($J_{C\text{-}F}$ = 36.0Hz), 114.26 ($J_{C\text{-}F}$ = 96.0Hz), m/z (ESI MS): calculated for $C_{16}H_9FNO_2S$ $(M+H)^+$: 298.03; obtained 298.1.

(4k) **3-(Benzo[d]thiazol-2-yl)-6-nitro-2H-chromen-2-one** (ECH-116): The title compound (**4k**) was obtained from the reaction of 2-hydroxy-5-nitrobenzaldehyde (**1k**) with 2-benzothaizoleacetonitrile as a brown solid in 67% yield by following the general procedure. ^{1}H NMR (400MHz, $CDCl_3$) δ (ppm): 9.15 (s, 1H), 8.67 (d, *J* = 4.0 Hz, 1H), 8.49 (dd, *J* = 4.0 & 8.0 Hz, 1H), 8.13 (d, *J* = 8.0 Hz, 1H), 8.02 (d, *J* = 8.0 Hz, 1H), 7.56-7.60 (m, 2H), 7.48 (t, *J* = 8.0Hz, 1H); ^{13}C NMR (100MHz, DMSO-d_6) δ (ppm): 166.54, 162.50, 155.14, 151.70, 144.06, 136.08, 126.71, 126.20, 125.87, 124.89, 124.10, 123.21, 121.80, 118.37, 118.09, 116.41; m/z (ESI MS): not ionised.

(4l) **10-(Benzo[d]thiazol-2-yl)-2,3,6,7-tetrahydro-1H-pyrano[2,3-f]pyrido[3,2,1-ij]quinolin-11(5H)-one** (ECH-117): The title compound (**4l**) was obtained from the reaction of 9-formyl-8-hydroxyjulolidine (**1l**) with 2-benzothaizoleacetonitrile as a brown solid in 63% yield by following the general procedure. ^{1}H NMR (400MHz, DMSO-d_6) δ (ppm): 8.86 (s, 1H), 8.10 (d, *J* = 8.0 Hz, 1H), 7.97 (d, *J* = 8.0 Hz, 1H), 7.51 (t, *J* = 8.0 Hz, 1H), 7.36-7.41 (m, 2H); ^{13}C NMR (150 MHz, DMSO-d_6) δ (ppm): 161.91, 160.85, 152.64, 152.05, 148.31, 142.68, 135.74, 127.68, 126.68, 124.76, 122.36, 122.07, 120.06, 109.59, 108.24, 105.41, 50.05, 49.51, 27.34, 21.01, 20.07, 20.05; m/z (HRMS): calculated for $C_{22}H_{18}N_2NaO_2S$ $(M+Na)^+$: 397.0991; obtained 397.0995. HPLC purity 99.60%.

(4m) **2-(Benzo[d]thiazol-2-yl)-3H-benzo[f]chromen-3-one** (ECH-118): The title compound (**4m**) was obtained from the reaction of 2-hydroxy-1-naphthaldehyde (1m) with 2-benzothaizoleacetonitrile as a yellow solid in 77% yield by following the general procedure. ^{1}H NMR (400MHz, $CDCl_3$) δ (ppm): 10.01 (s, 1H), 8.65 (d, *J* = 8.0 Hz, 1H), 8.20 (d, *J* = 8.0 Hz, 1H), 8.12 (d, *J* = 8.0 Hz, 1H), 8.01 (d, *J* = 8.0 Hz, 1H), 7.96 (d, *J* = 8.0 Hz, 1H), 7.81 (t, *J* = 8.0 Hz, 1H), 7.65 (t, *J* = 8.0 Hz, 1H), 7.55-7.60 (m, 2H), 7.46 (t, *J* = 8.0 Hz, 1H); ^{13}C NMR (150MHz, DMSO-d_6) δ (ppm): 160.40, 159.90, 154.25, 151.97, 137.77, 136.59, 135.17, 130.52, 129.62, 129.16, 128.99, 126.71, 126.70, 125.50, 122.69, 122.33, 121.84, 118.67, 116.62, 113.67; m/z (ESI MS): calculated for $C_{20}H_{12}NO_2S$ $(M+H)^+$: 330.06; obtained 330.1.

Procedure for synthesis of (4n) **6-amino-3-(benzo[d]thiazol-2-yl)-2H-chromen-2-one** (ECH-119): To a stiring solution of 3-(benzo[d]thiazol-2-yl)-6-nitro-2H-chromen-2-one (**4k**) in 25 mL of methanol, 10% activated Pd/C was added slowly and the reaction mixture was stirred for 6 h

under a H_2 gas atmosphere. Progress of the reaction was monitored through TLC and upon complete disappearance of **4k**, the reaction mixture was filtered through a bed of celite. The filtrate was then concentrated under reduced pressure to give the desired 6-amino-3-(benzo[d]thiazol-2-yl)-2H-chromen-2-one derivative (**4n**) in 86% yield. ^{1}H NMR (400MHz, DMSO-d_6) δ (ppm): 9.08 (s, 1H), 8.19 (d, J = 8.0 Hz, 1H), 8.10 (d, J = 8.0 Hz, 1H), 7.59 (t, J = 8.0 Hz, 1H), 7.49 (t, J = 8.0 Hz, 1H), 7.28 (d, J = 8.0 Hz, 1H), 7.01-7.05 (m, 2H), 5.43 (s, 2H); ^{13}C NMR (100MHz, DMSO-d_6) δ (ppm): 160.60, 160.20, 152.38, 146.73, 145.79, 142.76, 136.41, 127.11, 125.81, 122.94, 122.68, 121.52, 119.64, 119.27, 117.11, 111.41; ; m/z (HRMS): calculated for $C_{16}H_{11}N_2O_2S$ $(M+H)^+$: 295.0536; obtained 295.0544.

(5a) **3-(1H-Benzo[d]imidazol-2-yl)-7-(diethylamino)-2H-chromen-2-one** (ECH-120): The title compound (**5a**) was obtained from the reaction of 4-(diethylamino)-2-hydroxybenzaldehyde (**1a**) with 2-benzimidazoleacetonitrile as a greenish brown solid in 63% yield by following the general procedure. ^{1}H NMR (400MHz, $CDCl_3$) δ (ppm): 11.30 (brs, 1H), 9.09 (s, 1H), 7.65 (brs, 2H), 7.51 (d, J = 8.0 Hz, 1H), 7.29-7.31 (m, 2H), 6.69 (d, J = 8.0 Hz, 1H) 6.56 (s, 1H), 3.48 (q, J = 4.0 & 8.0 Hz, 4H), 1.26 (t, J = 8.0Hz, 6H); ^{13}C NMR (100MHz, $CDCl_3$) δ (ppm):162.02, 156.96,152.24, 147.74, 143.54, 130.80, 123.12, 110.24, 108.85, 96.91, 45.15, 12.47; m/z (ESI MS): calculated for $C_{20}H_{20}N_3O_2$ $(M+H)^+$: 334.16; obtained 334.2.

(5b) **10-(1H-Benzo[d]imidazol-2-yl)-2,3,6,7-tetrahydro-1H-pyrano[2,3-f]pyrido[3,2,1-ij]quinolin-11(5H)-one** (ECH-121): The title compound (**5b**) was obtained from the reaction of 9-formyl-8-hydroxyjulolidine (**1l**) with 2-benzimidazoleacetonitrile as a greenish brown solid in 65% yield by following the general procedure. ^{1}H NMR (400MHz, DMSO-d_6) δ (ppm): 8.99 (s, 1H), 7.75-7.78 (m, 2H), 7.43-7.45 (m, 2H), 7.15 (s, 1H), 3.31.3.36 (m, 4H), 2.73-2.79 (m, 4H), 1.85-1.92 (m, 4H); ^{13}C NMR (100MHz, DMSO-d_6) δ (ppm): 159.58, 152.42, 149.62, 146.34, 145.49, 132.86, 127.66, 125.26, 120.88, 114.31, 108.06, 105.60, 99.43, 50.26, 49.72, 27.05, 20.77, 19.89, 19.80; m/z (ESI MS): calculated for $C_{22}H_{20}N_3O_2$ $(M+H)^+$: 358.16; obtained 358.2.

General procedure for preparation of quaternized coumarin-benzothaizole 6(a-b) and coumarin-benzoimidazole (6c-d) derivatives: To a mixture of compound (**4a**,**l** or **5a-b**) (30 mg, 0.016-0.041 mmol) in 3 mL of dichloroethane was added methyl iodide (0.3 mL, 4.82 mmol) in a sealed microwave vial. The reaction mixture was then irradiated under MW

conditions at 125 °C for 1h. The reaction mixture was filtered through sintered funnel and washed with DCM (5 mL), followed by water (1 mL) and diethyl ether (5 mL). The solid was then dried under vacuum to give the desired quaternized coumarin-benzothaizole **6(a-b)** and coumarin-benzoimidazole (**6c-d**) derivatives in pure form with 82-87% yields.

(6a) **2-(7-(Diethylamino)-2-oxo-2H-chromen-3-yl)-3-methylbenzo[d]thiazol-3-ium iodide** (ECH-122): The title compound (**6a**) was obtained from the reaction of 3-(Benzo[*d*]thiazol-2-yl)-7-(diethylamino)-2*H*-chromen-2-one (**4a**) with methyl iodide as a yellow solid in 86% yield by following the general procedure. ^{1}H NMR (400MHz, DMSO-d_6) δ (ppm): 8.77 (s, 1H), 8.45 (d, J = 8.0 Hz, 1H), 8.32 (d, J = 8.0 Hz, 1H), 7.92 (t, J = 8.0 Hz, 1H), 7.78-7.83 (m, *2*H), 6.99 (d, J = 8.0 Hz, 1H) 6.78 (s, 1H), 4.35 (s, 3H), 3.60 (q, J = 8.0 & 8.0 Hz, 4H), 1.20 (t, J = 8.0Hz, 6H); ^{13}C NMR (100MHz, DMSO-d_6) δ (ppm): 168.74, 159.31, 158.19, 154.81, 149.38, 142.23, 133.55, 129.88, 129.73, 128.45, 124.52, 117.21, 111.83, 108.57, 103.83, 96.94, 45.36, 39.67, 12.91; m/z (ESI MS): calculated for $C_{21}H_{21}N_2O_2S$ $(M)^+$: 365.1318; obtained 365.1327.

(6b) **3-Methyl-2-(11-oxo-2,3,5,6,7,11-hexahydro-1H-pyrano[2,3-f]pyrido[3,2,1-ij]quinolin-10-yl)benzo[d]thiazol-3-ium iodide** (ECH-123): The title compound (**6b**) was obtained from the reaction of 10-(benzo[*d*]thiazol-2-yl)-2,3,6,7-tetrahydro-1*H*-pyrano[2,3-*f*]pyrido[3,2,1-ij]quinolin-11(5*H*)-one (**4l**) with methyl iodide as a dark brown solid in 87% yield by following the general procedure. ^{1}H NMR (400MHz, DMSO-d_6) δ (ppm): 8.65 (brs, 1H), 8.40 (d, J = 8.0 Hz, 1H), 8.26 (d, J = 8.0 Hz, 1H), 7.88 (t, J = 8.0 Hz, 1H), 7.77 (t, J = 8.0 Hz, 1H), 7.40 (s, 1H), 4.33 (s, 3H), 3.47-3.50 (m, 4H), 2.77-2.81 (m, 4H), 1.91-1.96-3.50 (m, 4H); ^{13}C NMR (100MHz, DMSO-d_6) δ (ppm): 168.40, 159.68, 152.69, 151.13, 147.96, 142.25, 129.65, 129.42, 129.15, 128.09, 124.34, 121.46, 116.82, 108.57, 105.74, 101.66, 50.70, 50.12, 39.95, 27.13, 20.78, 19.76, 19.73; m/z (HRMS): calculated for $C_{23}H_{21}N_2O_2S$ $(M+H)^+$: 389.1318; obtained 389.1327. HPLC purity 96.38%.

(6c) **2-(7-(Diethylamino)-2-oxo-2H-chromen-3-yl)-1,3-dimethyl-1H-benzo[d]imidazol-3-ium iodide** (ECH-124): The title compound (**6c**) was obtained from the reaction of 3-(1*H*-benzo[*d*]imidazol-2-yl)-7-(diethylamino)-2*H*-chromen-2-one (**5a**) with methyl iodide as a yellow solid in 82% yield by following the general procedure. ^{1}H NMR (400MHz, DMSO-d_6) δ (ppm): 8.55 (s, 1H), 8.09-8.11 (m, 2H), 7.75-7.77 (m, 2H), 7.66 (d, J = 8.0 Hz, 1H), 6.92 (d, J = 8.0 Hz, 1H), 6.75 (s, 1H),

4.02 (s, 6H), 3.56 (q, J = 4.0 & 8.0 Hz, 4H), 1.19 (t, J = 8.0 Hz, 6H); ^{13}C NMR (100MHz, DMSO-d_6) δ (ppm): 158.54, 153.64, 151.37, 147.33, 132.23, 132.18, 127.20, 113.82, 110.81, 107.79, 99.25, 96.99, 45.06, 33.37, 12.84; m/z (HRMS): calculated for $C_{22}H_{25}N_3O_2$ $(M+H)^{2+}$: 363.1936; obtained 363.1937.

(6d) **1,3-dimethyl-2-(11-oxo-2,3,5,6,7,11-hexahydro-1H-pyrano[2,3-f]pyrido[3,2,1-ij]quinolin-10-yl)-1H-benzo[d]imidazol-3-ium iodide** (ECH-125): The title compound (**6d**) was obtained from the reaction of 10-(1*H*-benzo[*d*]imidazol-2-yl)-2,3,6,7-tetrahydro-1*H*-pyrano[2,3-*f*]pyrido[3,2,1-ij]quinolin-11(5*H*)-one (**5b**) with methyl iodide as a yellow solid in 85% yield by following the general procedure. ^{1}H NMR (400MHz, DMSO-d_6) δ (ppm): 8.39 (s, 1H), 8.08-8.10 (m, 2H), 7.74-7.76 (m, 2H), 7.25 (s, 1H), 3.99 (s, 6H), 3.41-3.43 (m, 4H), 2.76-2.83 (m, 4H), 1.89-1.96 (m, 4H); ^{13}C NMR (100MHz, DMSO-d_6) δ (ppm): 158.64, 153.22, 150.89, 149.35, 147.72, 132.18, 127.78, 127.11, 120.19, 113.75, 107.45, 105.60, 97.28, 50.20, 49.66, 33.33, 27.19, 20.97, 20.00; m/z (HRMS): calculated for $C_{24}H_{24}N_3O_2$: 386.1863; obtained 386.1872.

NMR Spectra

^{1}H & ^{13}C NMR of 3-(benzo[*d*]thiazol-2-yl)-7-(diethylamino)-2*H*-chromen-2-one (**4a**)

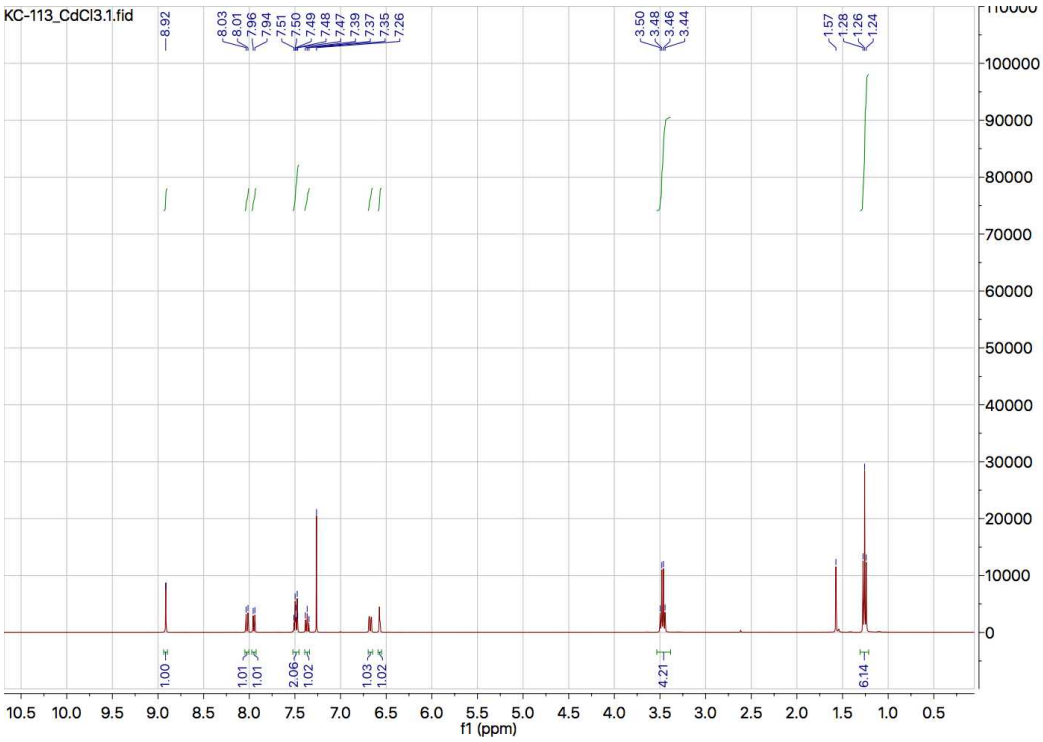

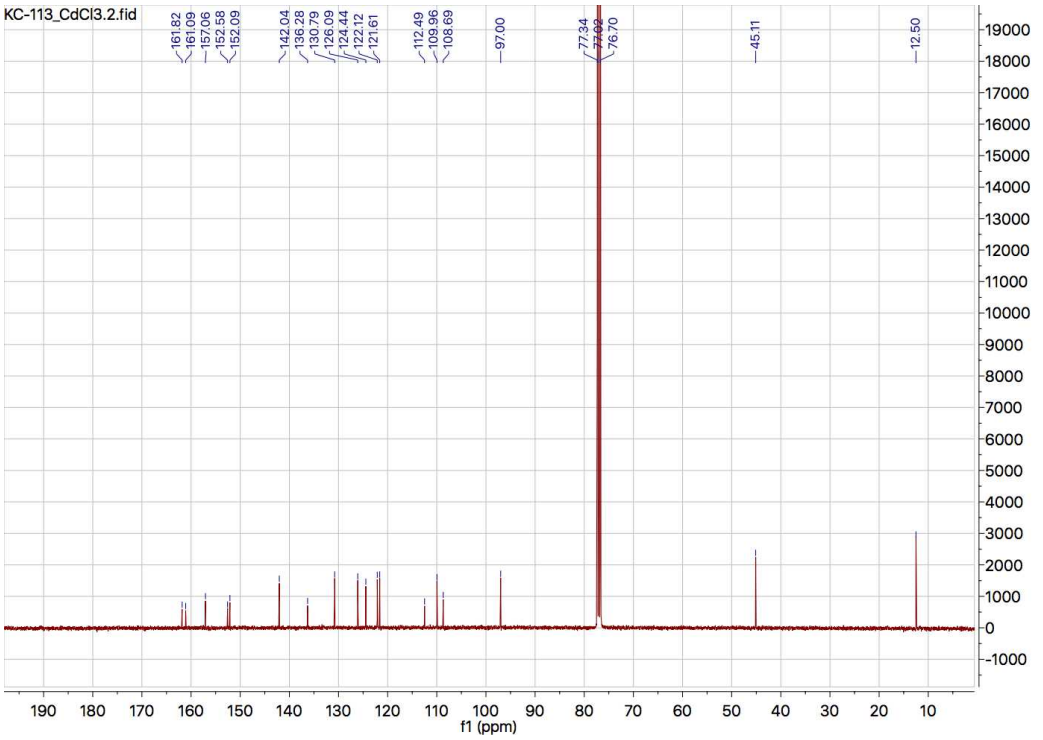

1H & 13C NMR of 3-(benzo[d]thiazol-2-yl)-7-hydroxy-2H-chromen-2-one (**4b**)

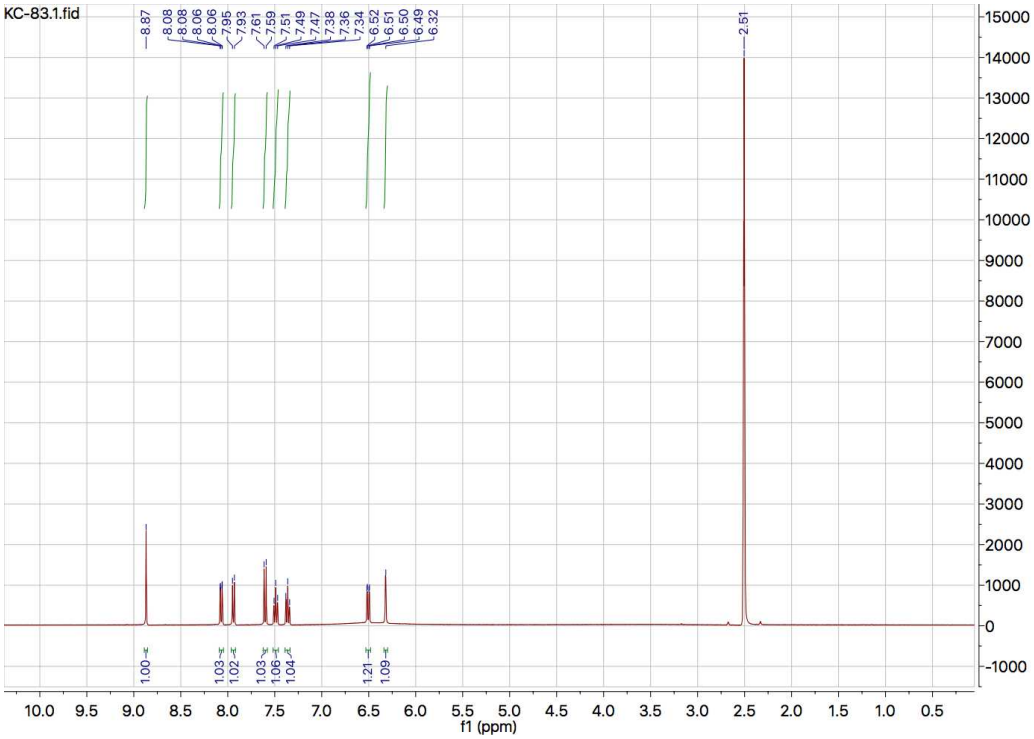

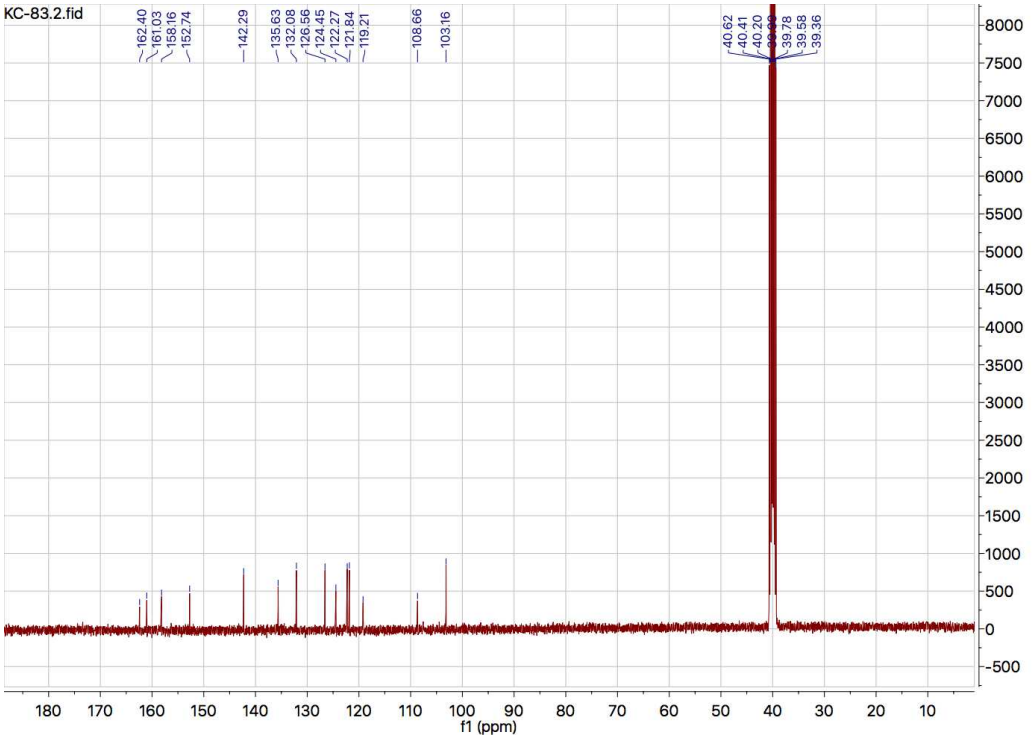

^{1}H & ^{13}C NMR of 3-(benzo[*d*]thiazol-2-yl)-7-methoxy-2H-chromen-2-one (**4c**).

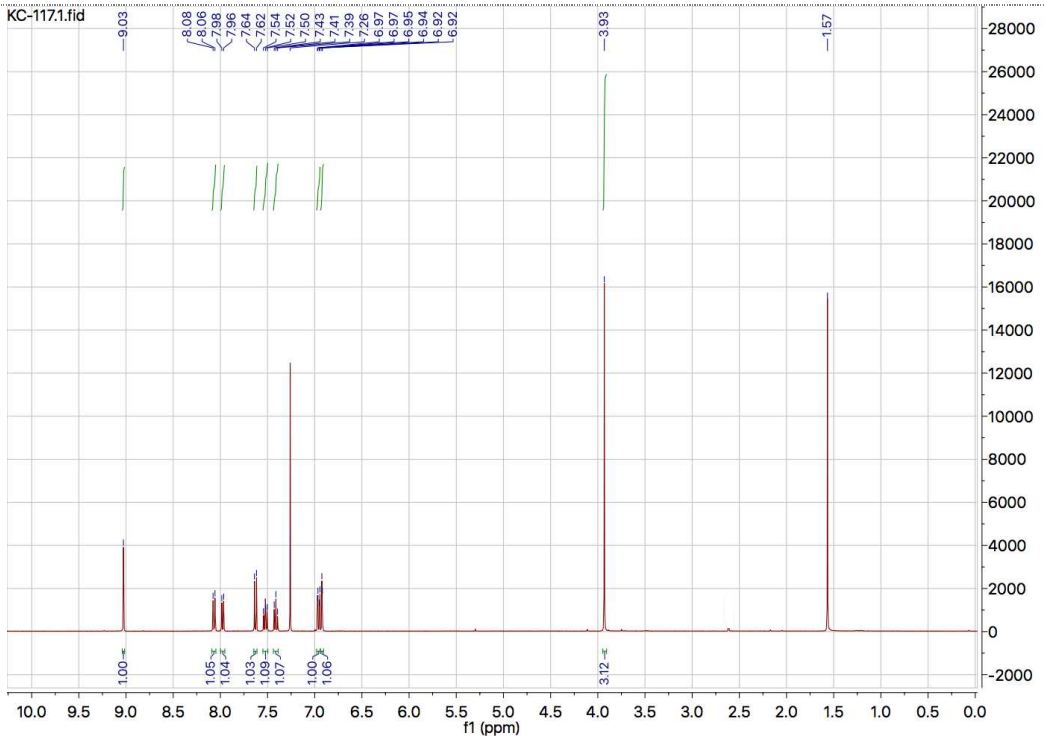

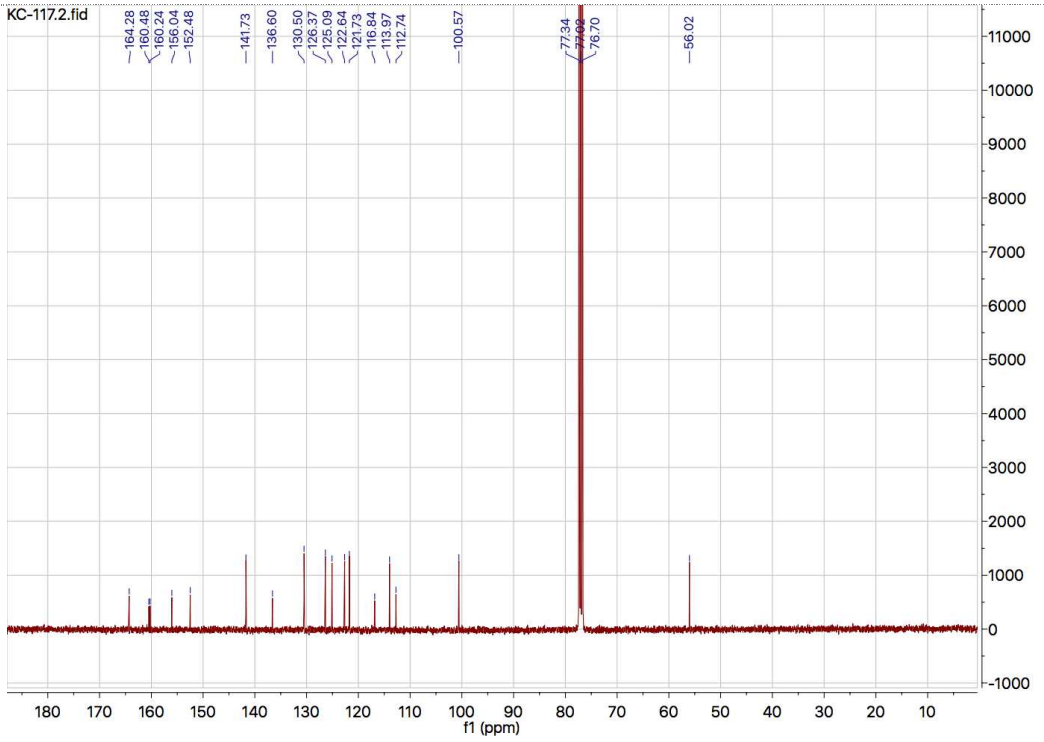

^{1}H & ^{13}C NMR of 3-(benzo[d]thiazol-2-yl)-2H-chromen-2-one (**4d**)

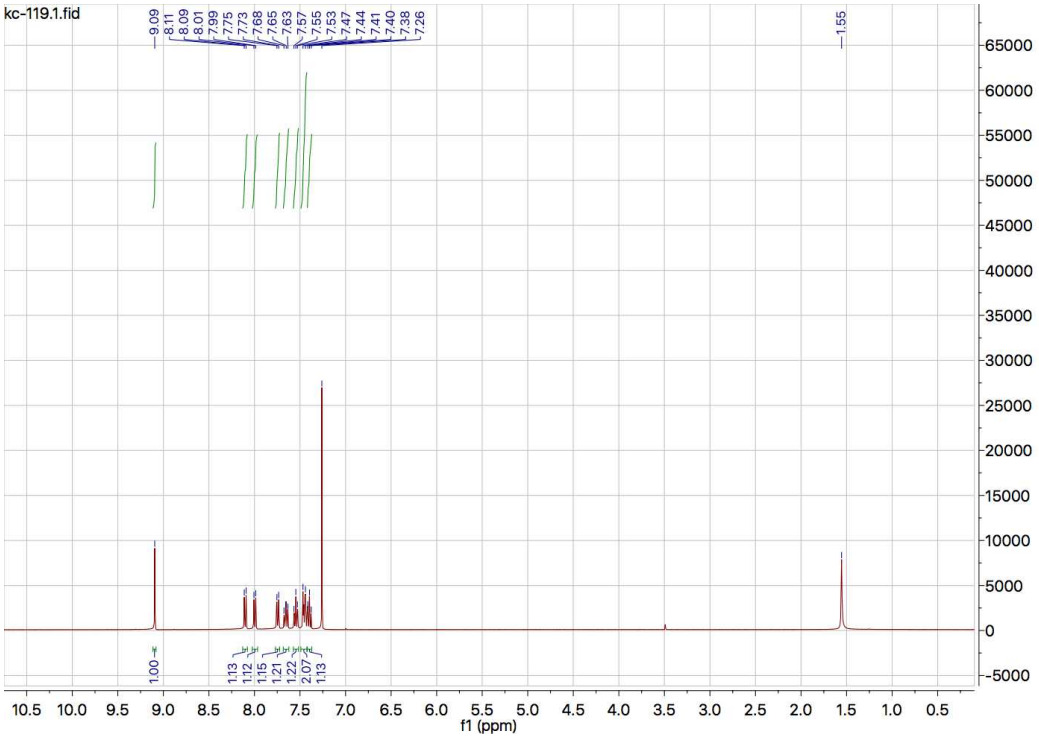

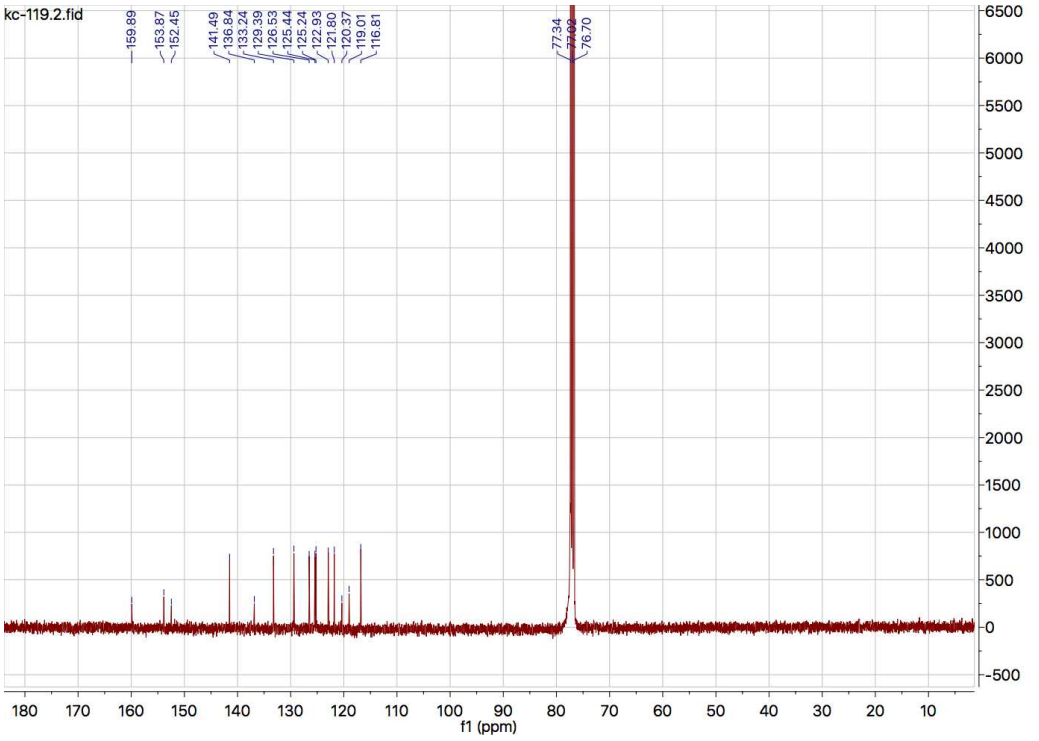

^{1}H & ^{13}C NMR of 3-(benzo[*d*]thiazol-2-yl)-8-methoxy-2*H*-chromen-2-one (**4e**)

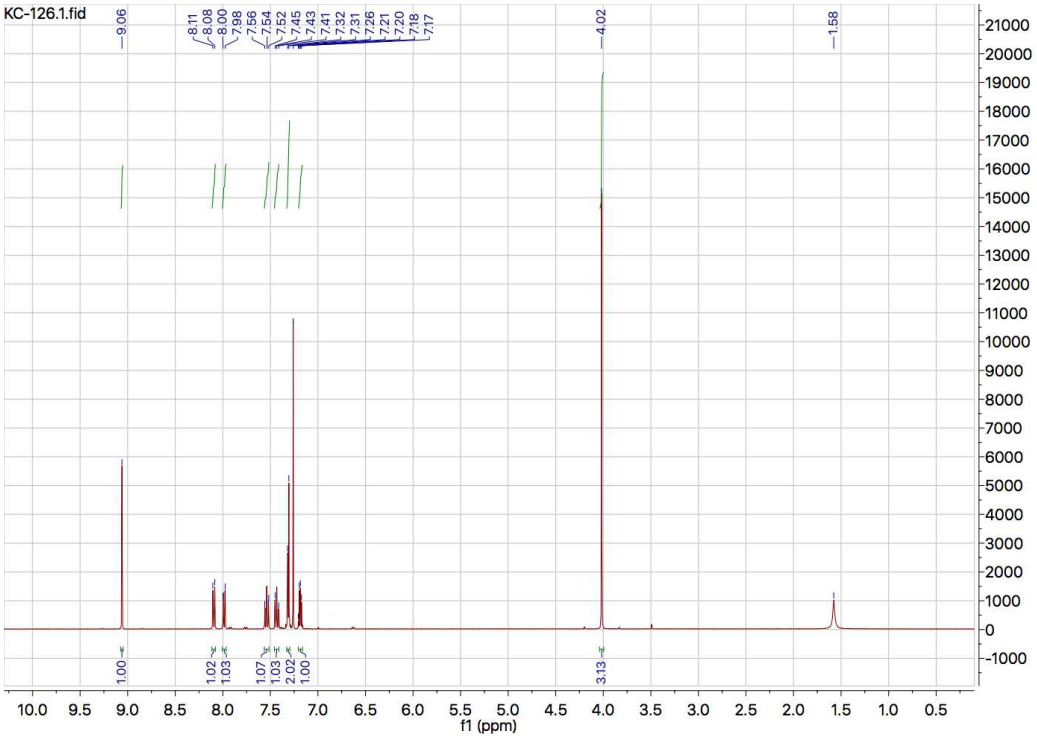

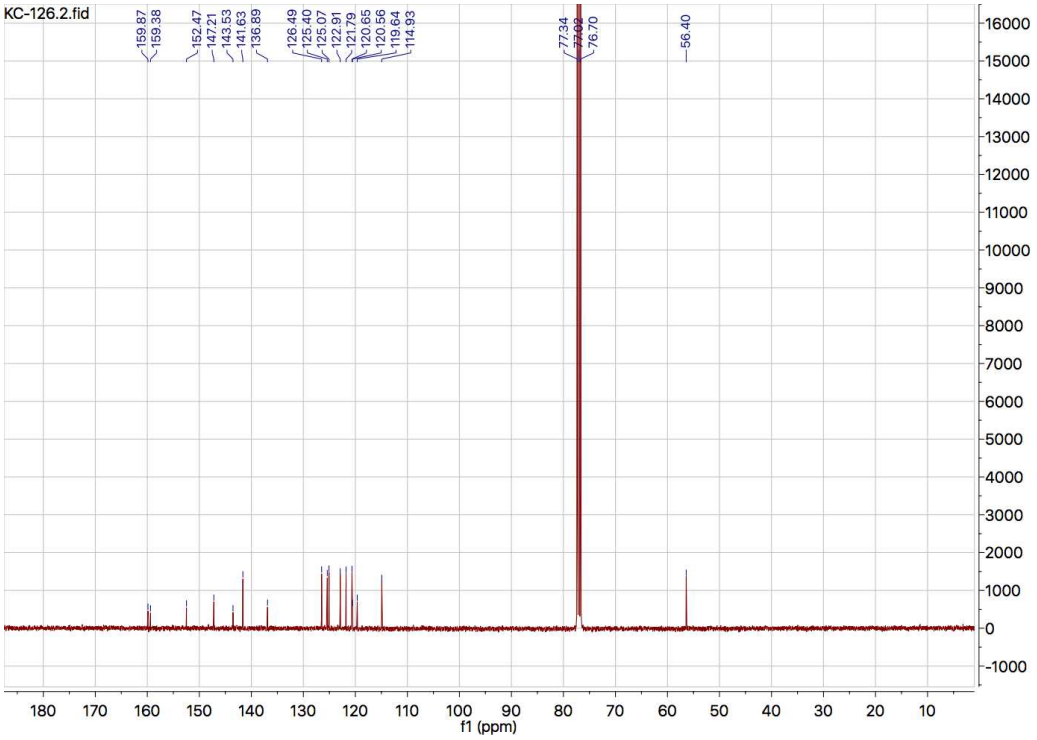

^{1}H & ^{13}C NMR of 3-(benzo[d]thiazol-2-yl)-8-hydroxy-2H-chromen-2-one (**4f**)

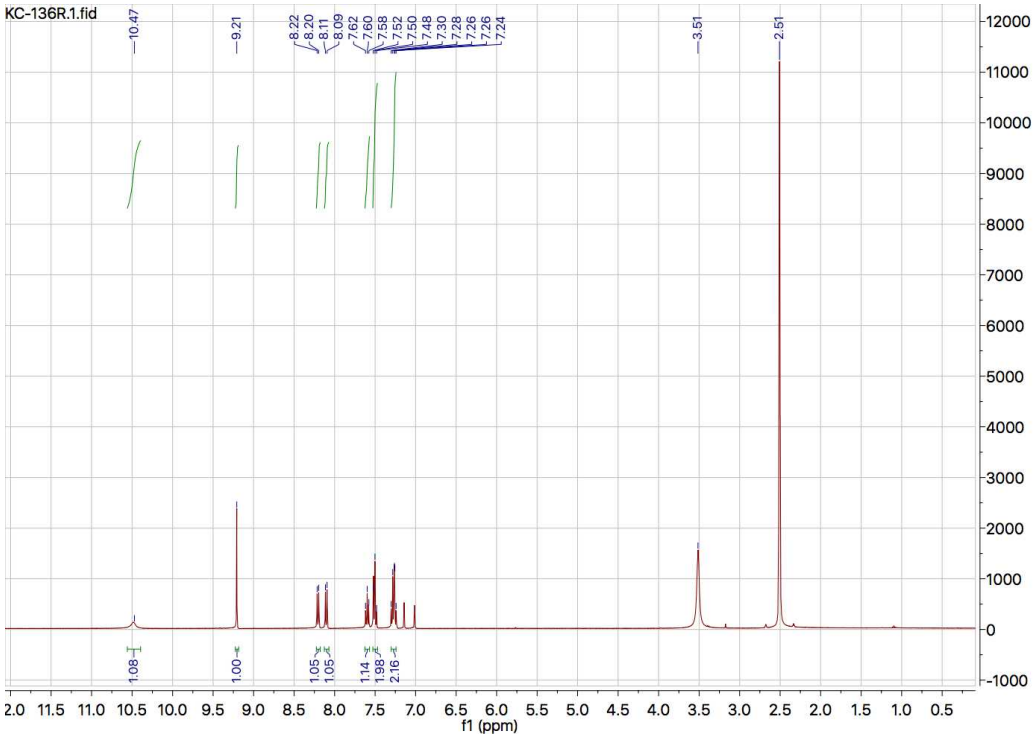

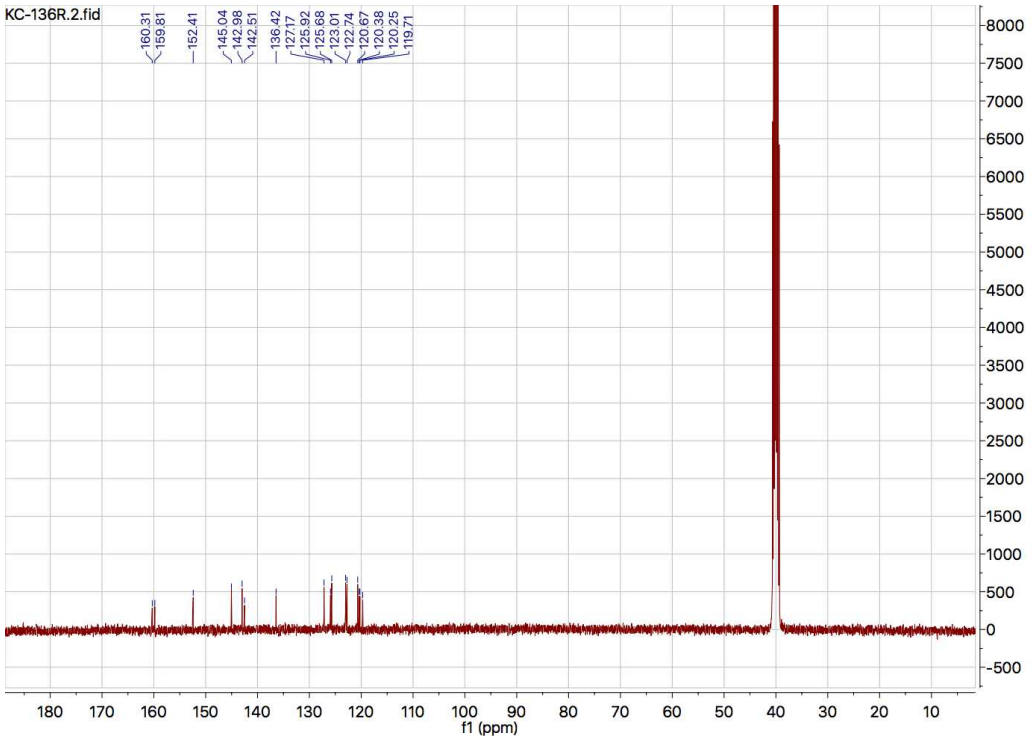

^{1}H & ^{13}C NMR of 3-(benzo[d]thiazol-2-yl)-8-nitro-2H-chromen-2-one (**4g**)

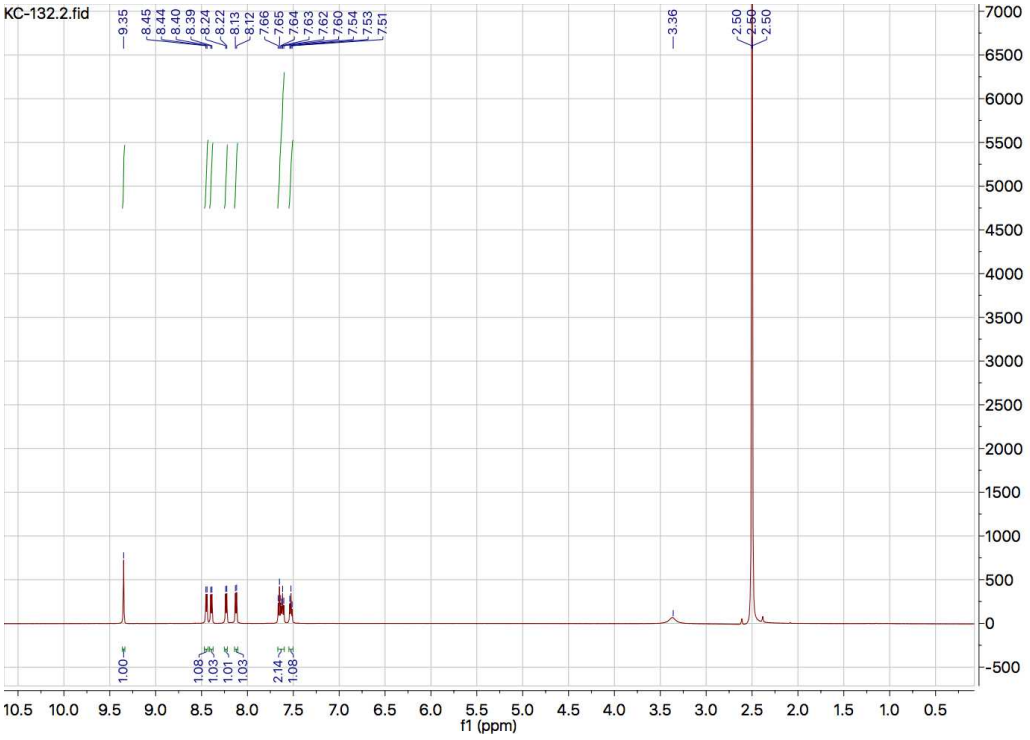

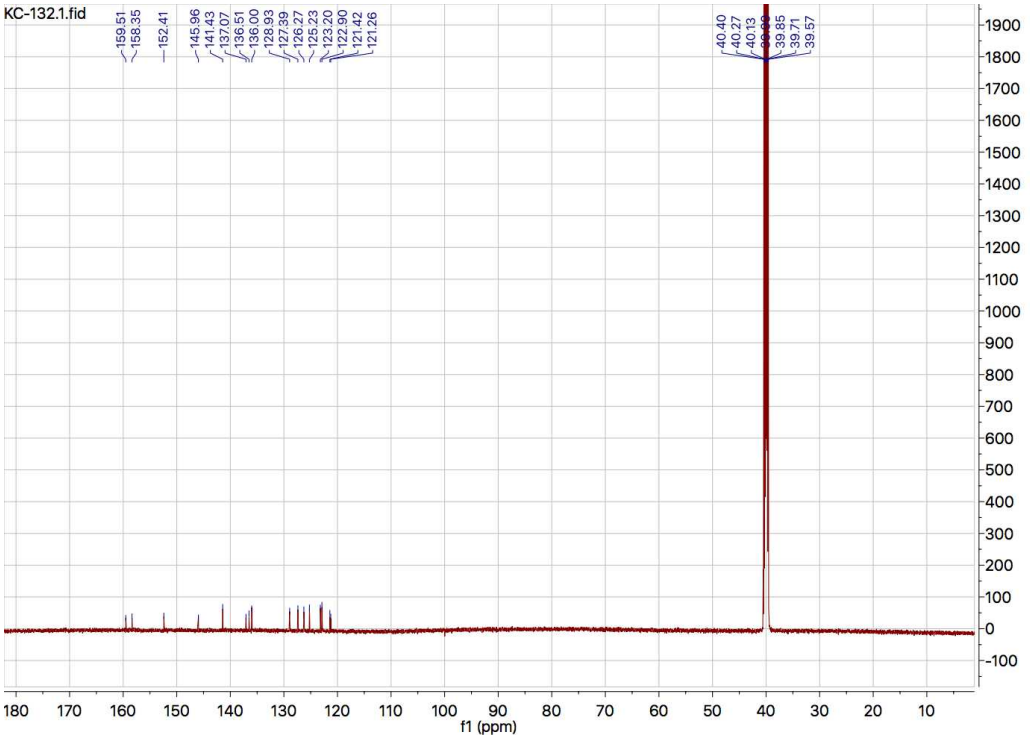

^{1}H & ^{13}C NMR of 3-(benzo[*d*]thiazol-2-yl)-6-methoxy-2H-chromen-2-one (**4h**)

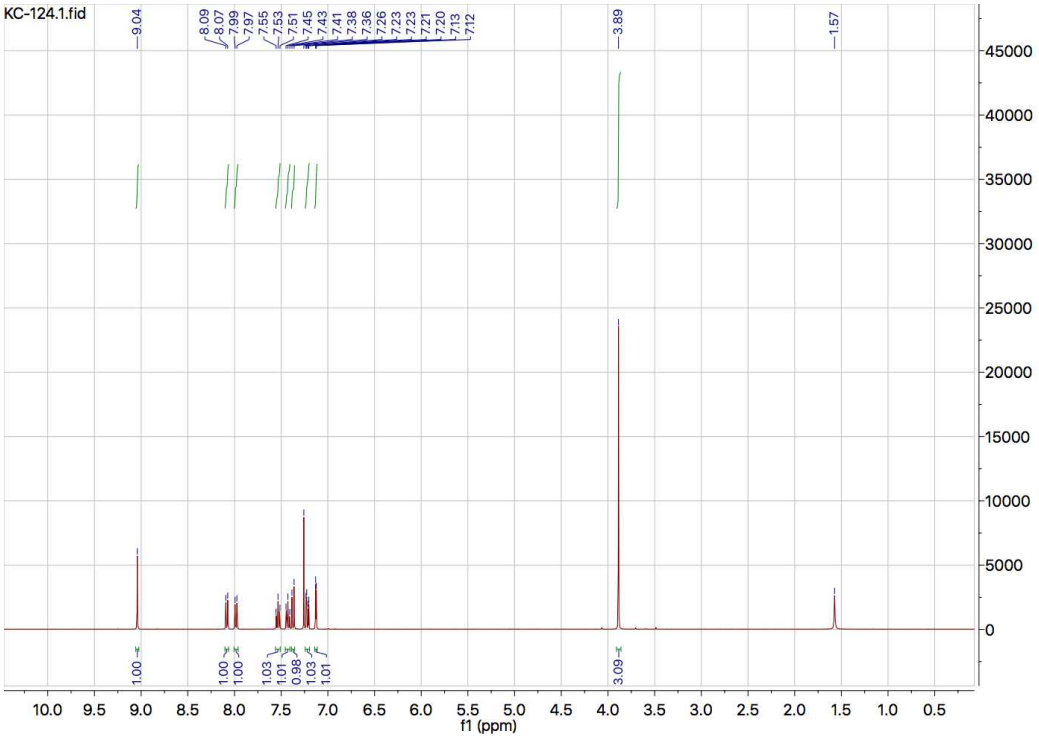

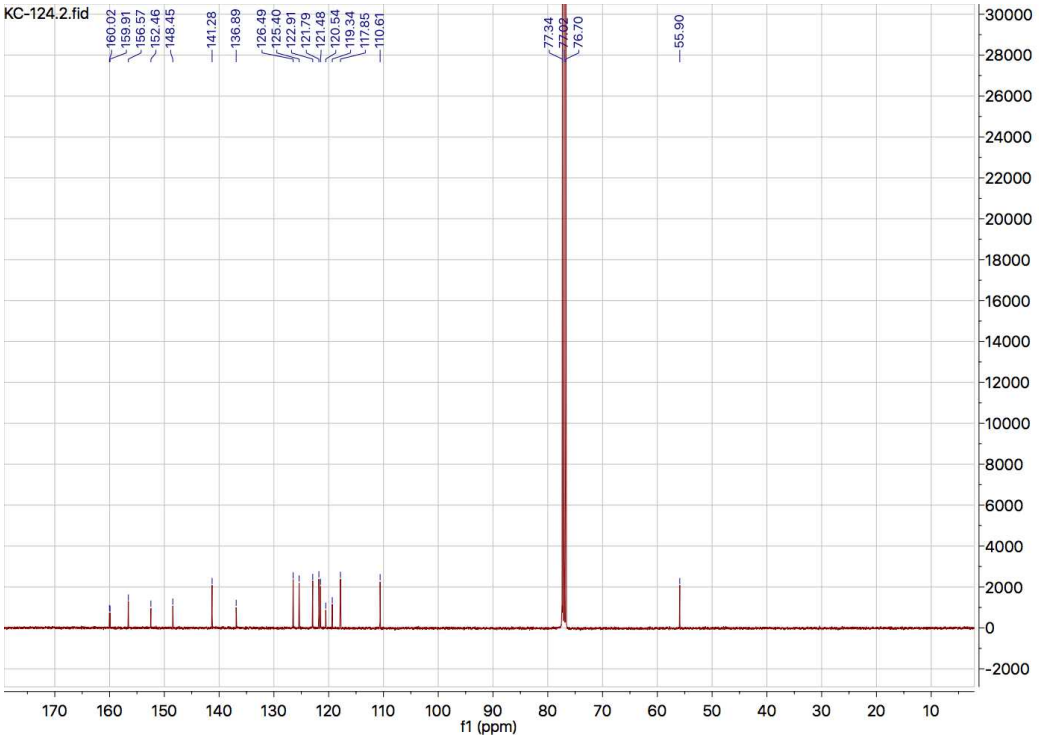

^{1}H & ^{13}C NMR of 3-(benzo[d]thiazol-2-yl)-6-hydroxy-2H-chromen-2-one (**4i**)

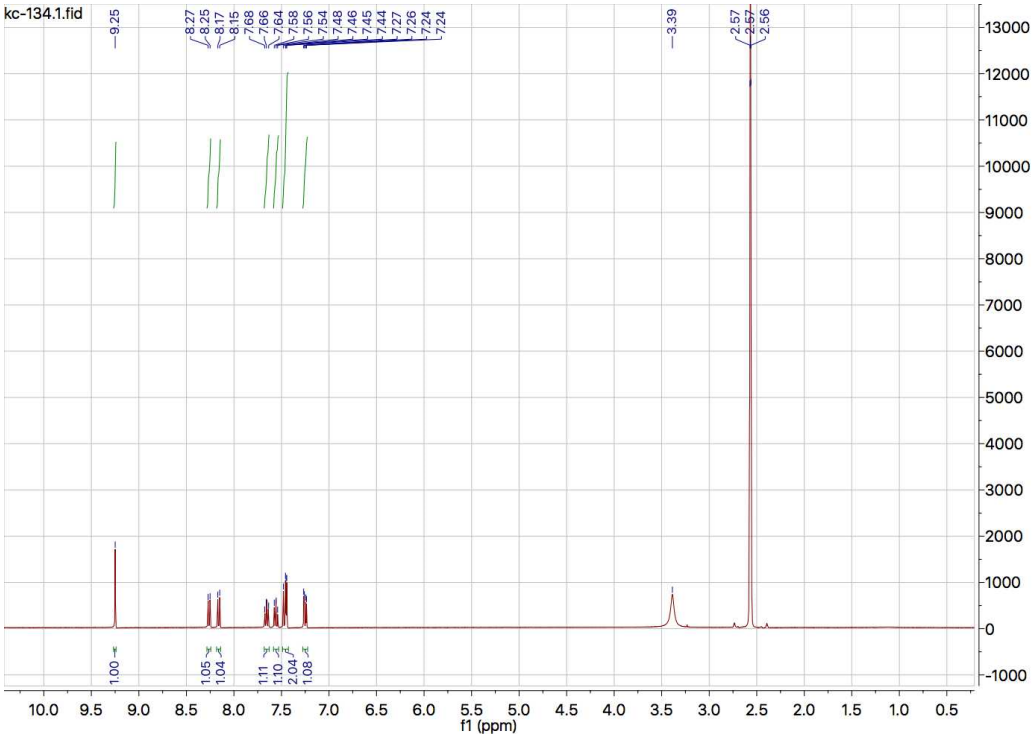

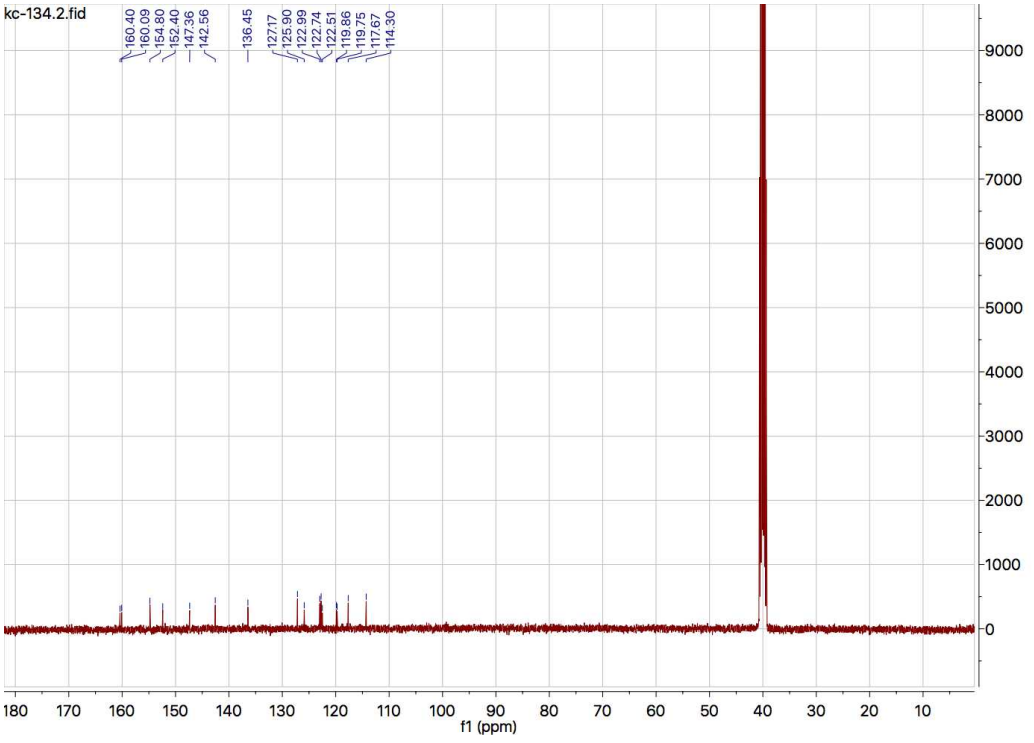

^{1}H & ^{13}C NMR of 3-(benzo[d]thiazol-2-yl)-6-fluoro-2H-chromen-2-one (**4j**)

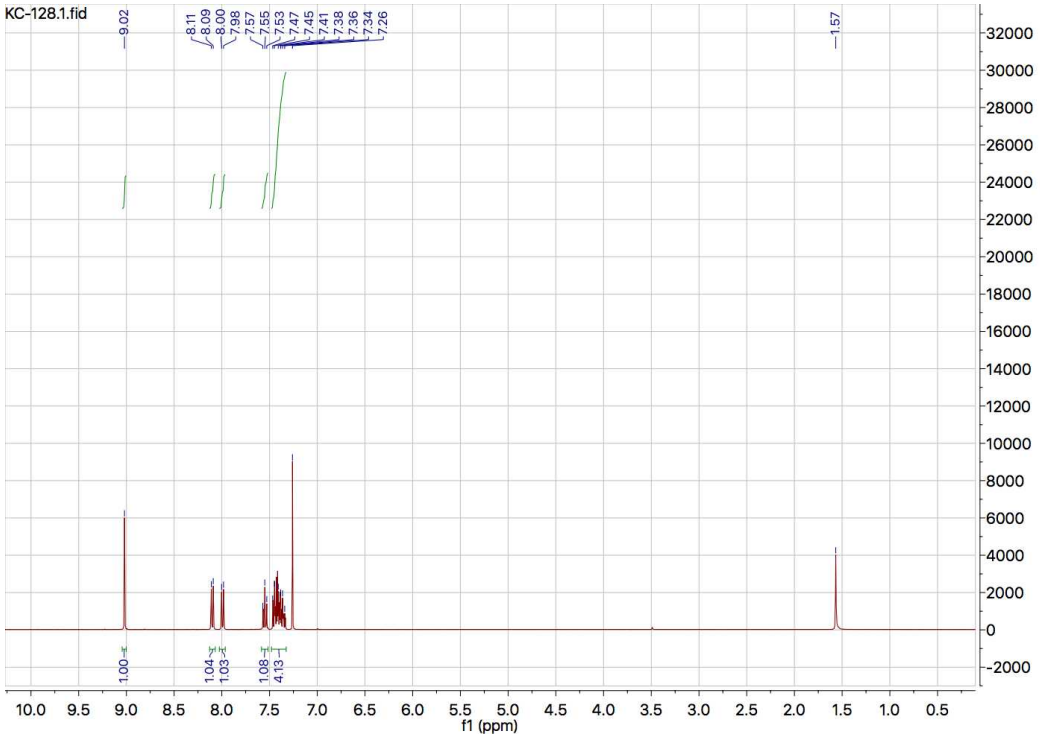

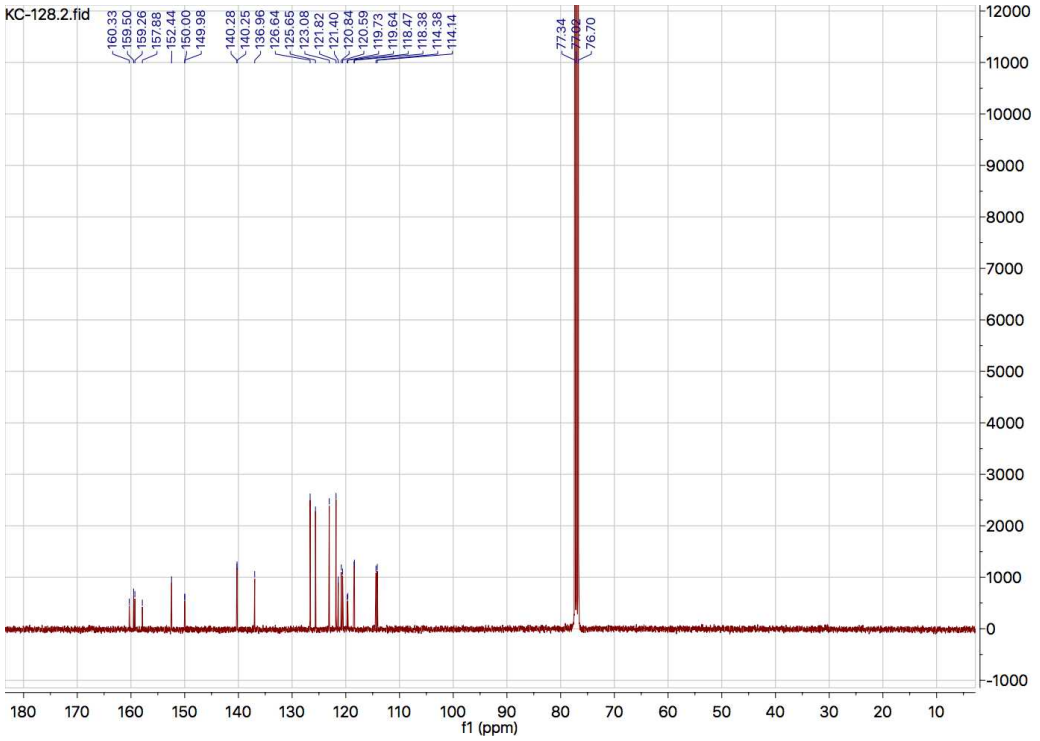

^{1}H & ^{13}C NMR of 3-(benzo[d]thiazol-2-yl)-6-nitro-2H-chromen-2-one (**4k**)

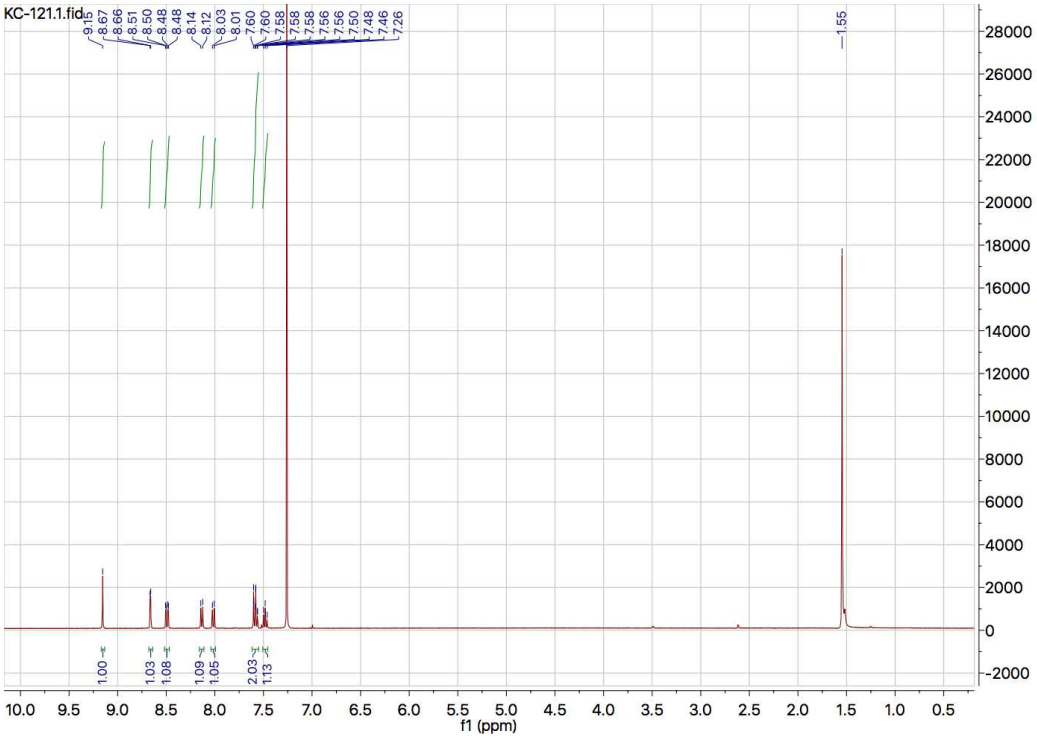

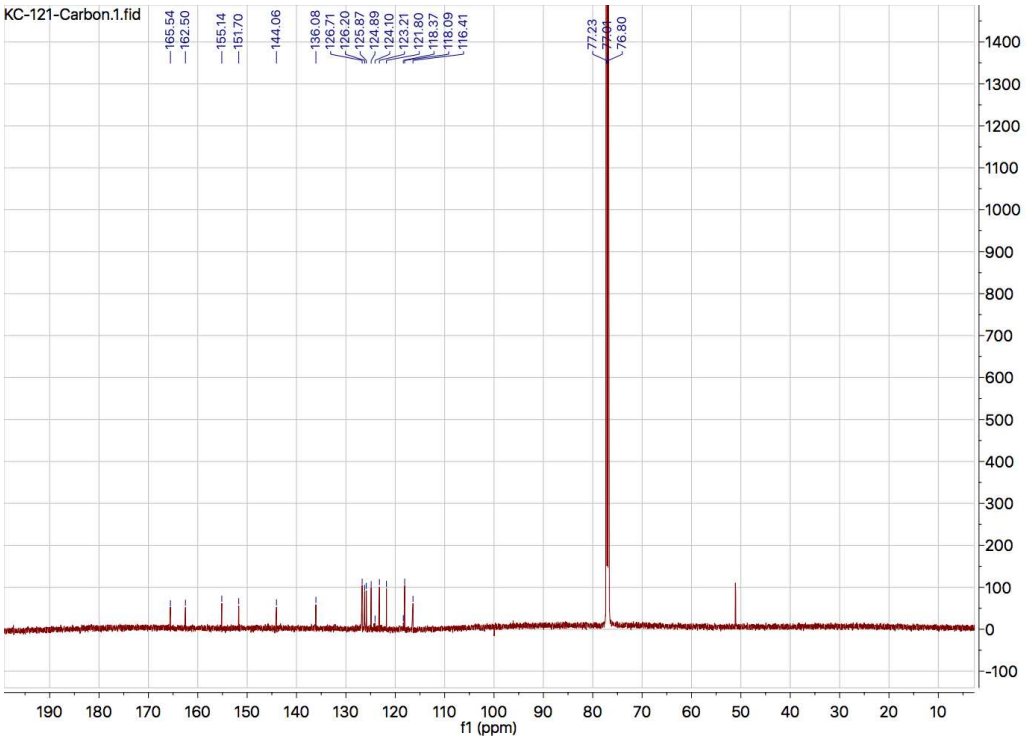

^{1}H & ^{13}C NMR of 10-(benzo[d]thiazol-2-yl)-2,3,6,7-tetrahydro-1H-pyrano[2,3-f]pyrido[3,2,1-ij]quinolin-11(5H)-one (**4l**)

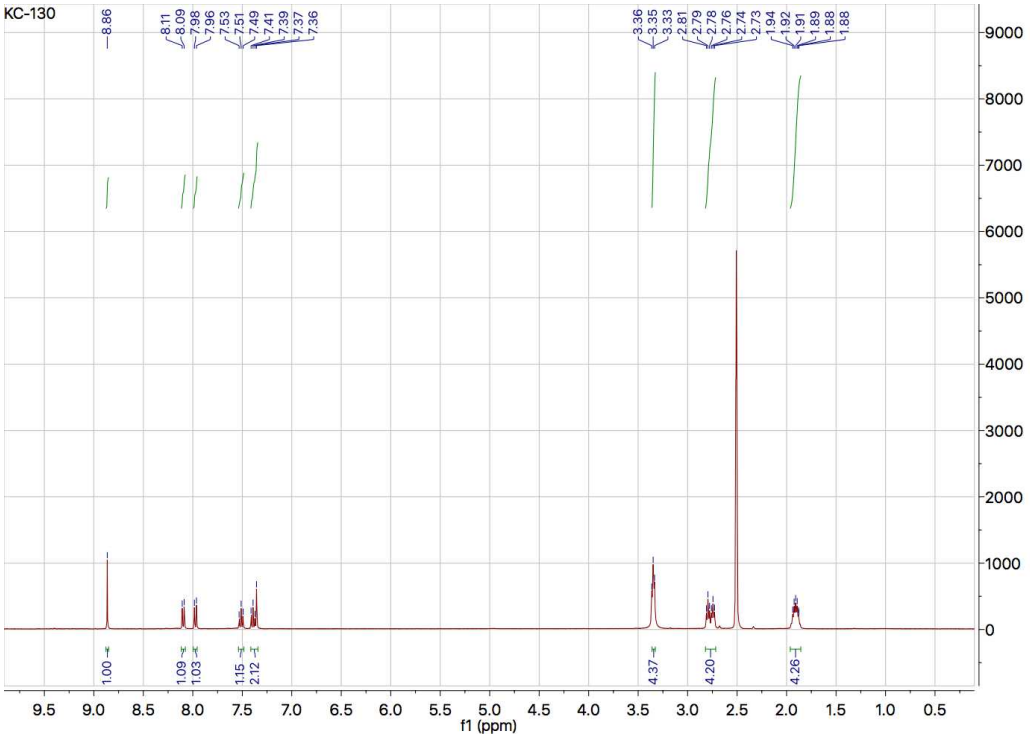

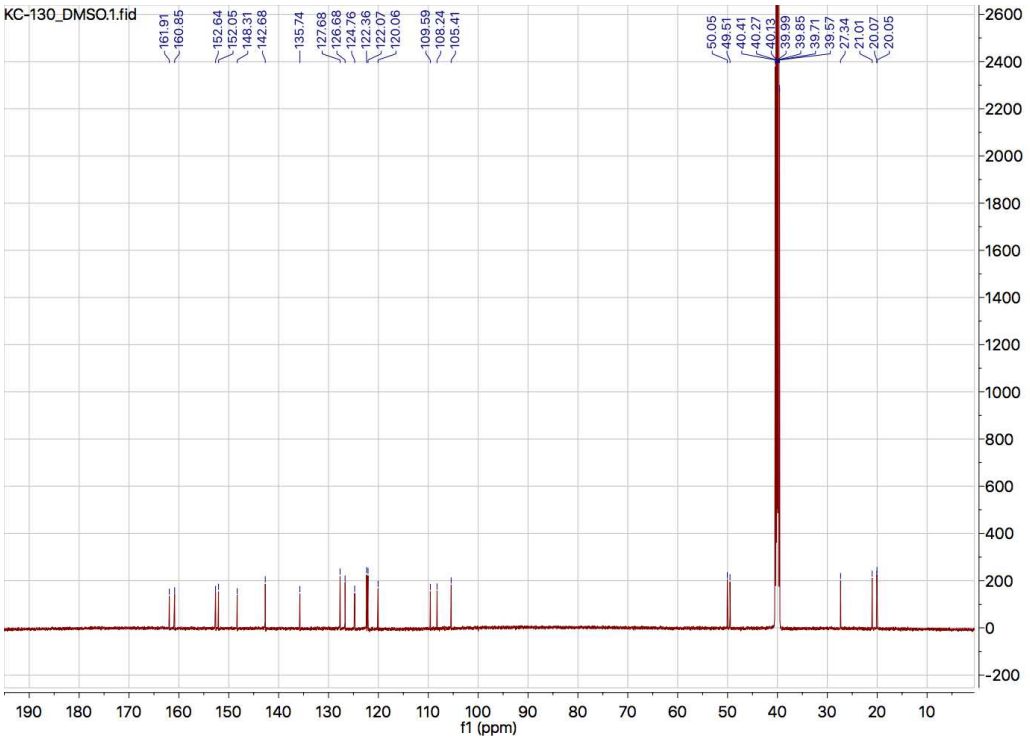

^{1}H & ^{13}C NMR of 2-(benzo[*d*]thiazol-2-yl)-3H-benzo[*f*]chromen-3-one **(4m)**

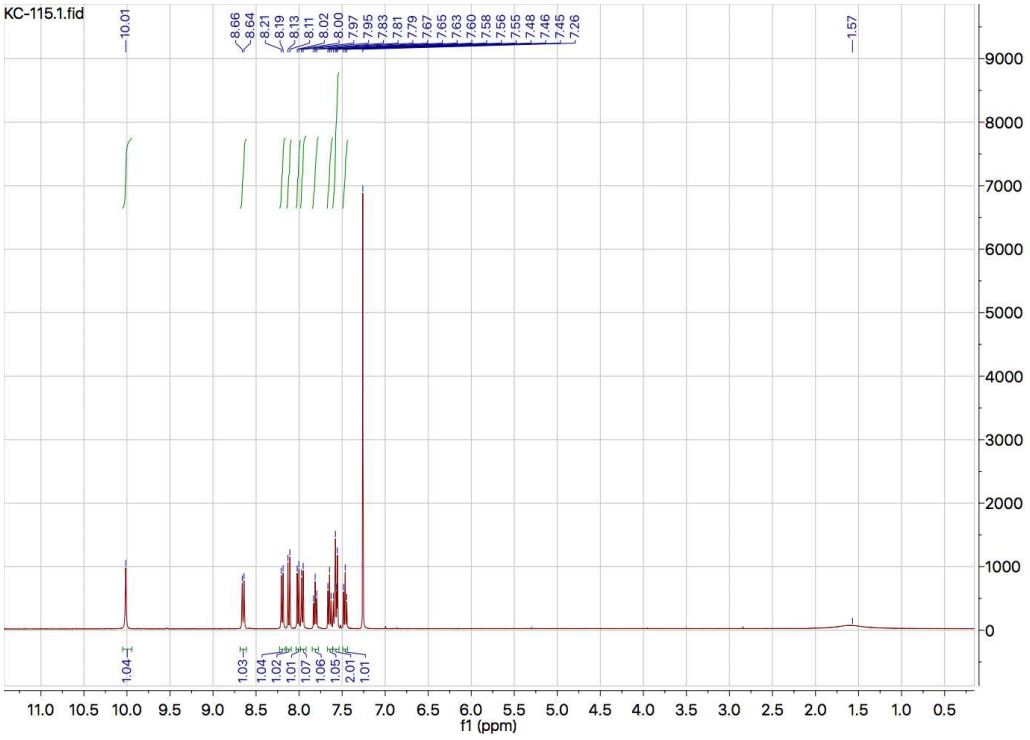

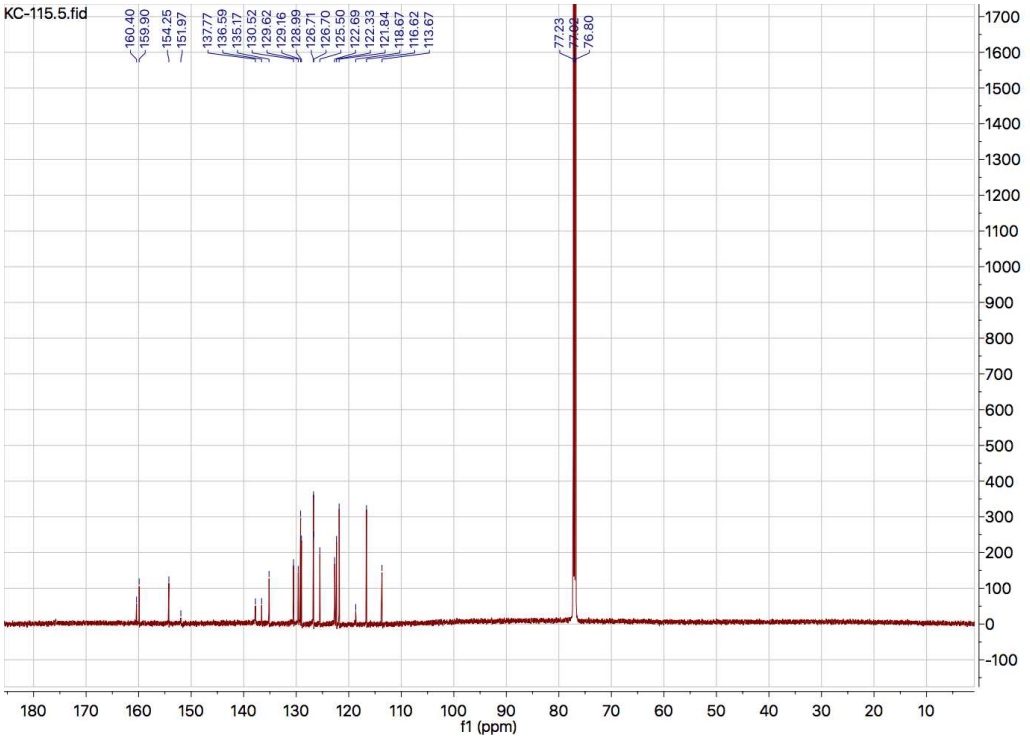

^{1}H & ^{13}C NMR of 6-amino-3-(benzo[d]thiazol-2-yl)-2H-chromen-2-one (**4n**)

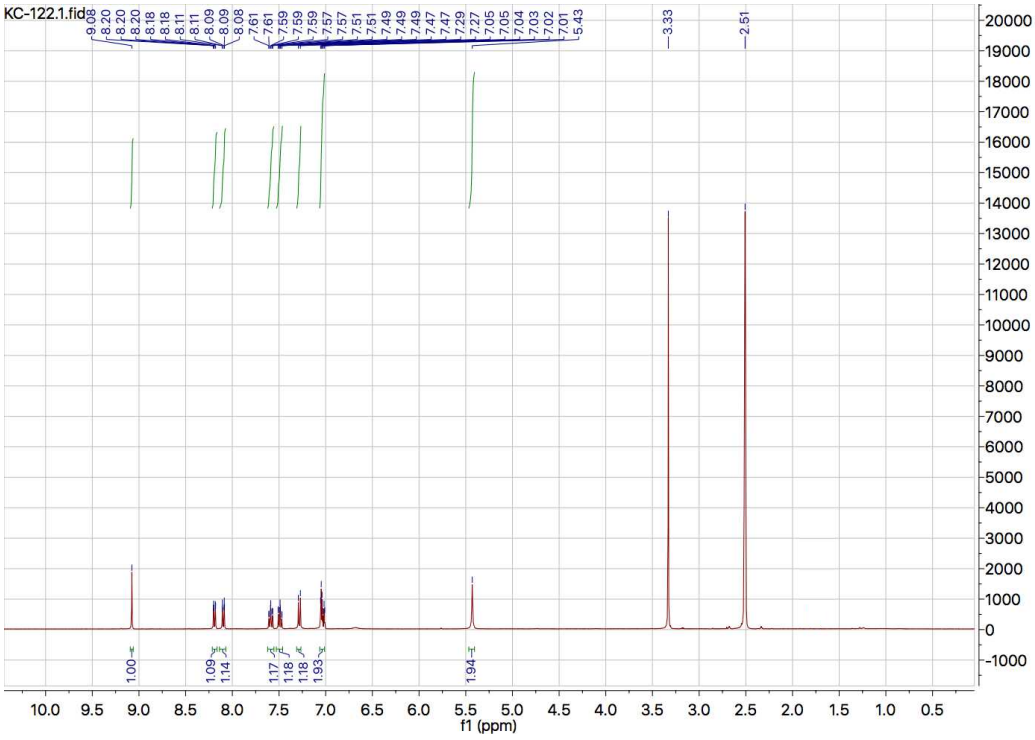

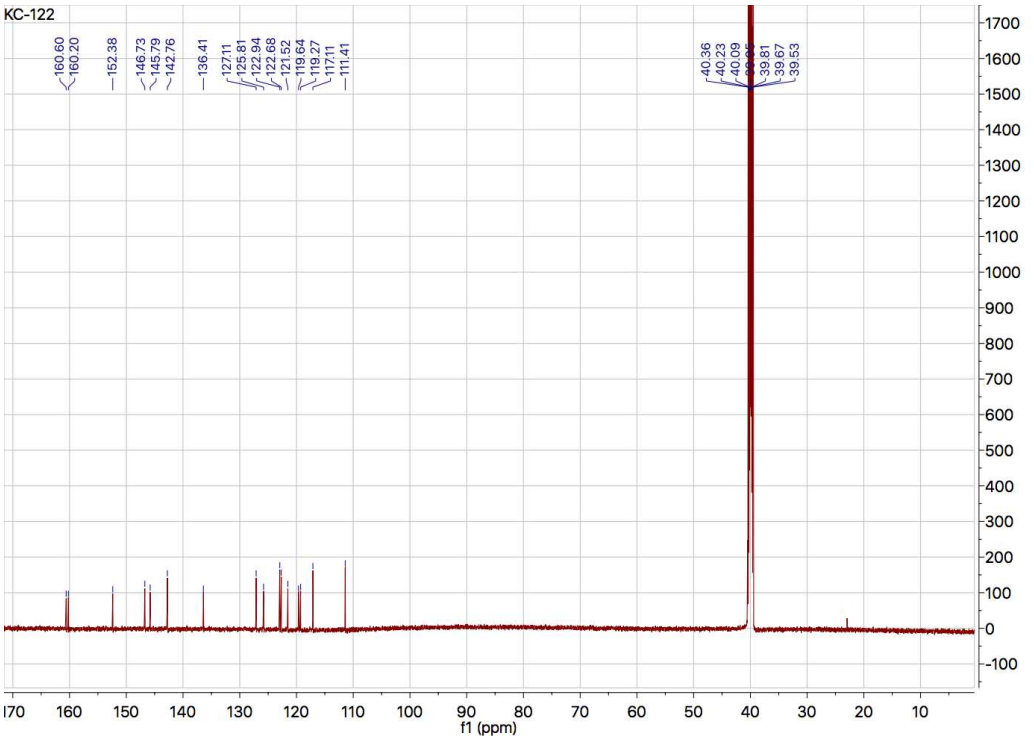

^{1}H & ^{13}C NMR of 3-(1*H*-benzo[d]imidazol-2-yl)-7-(diethylamino)-2H-chromen-2-one (**5a**)

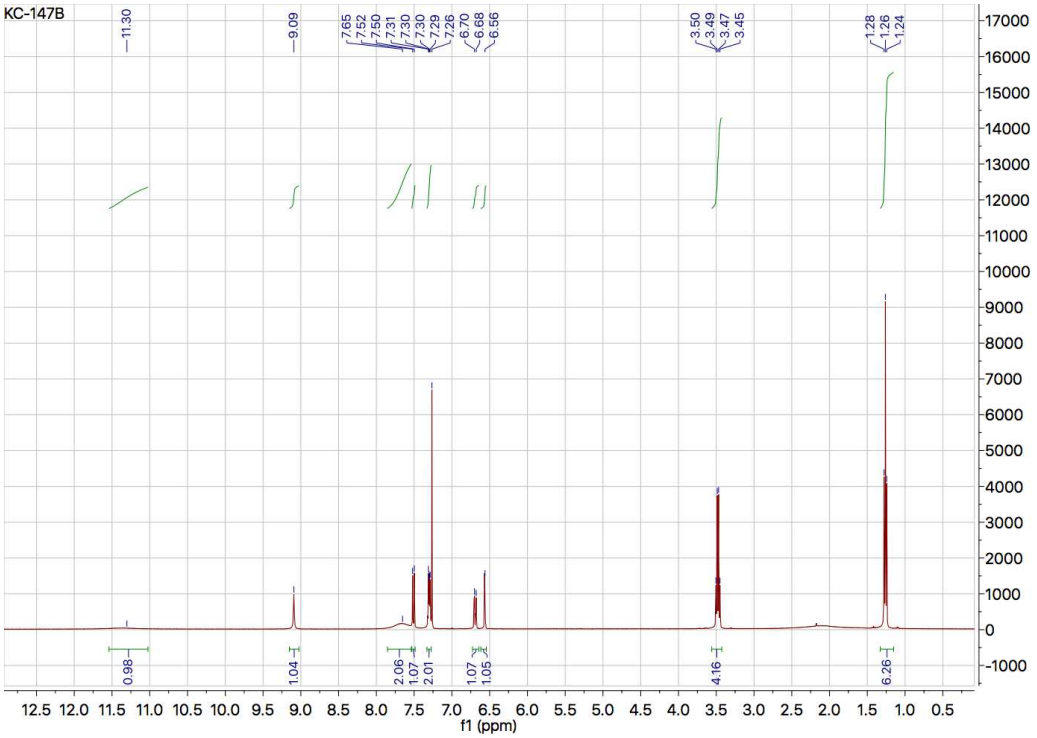

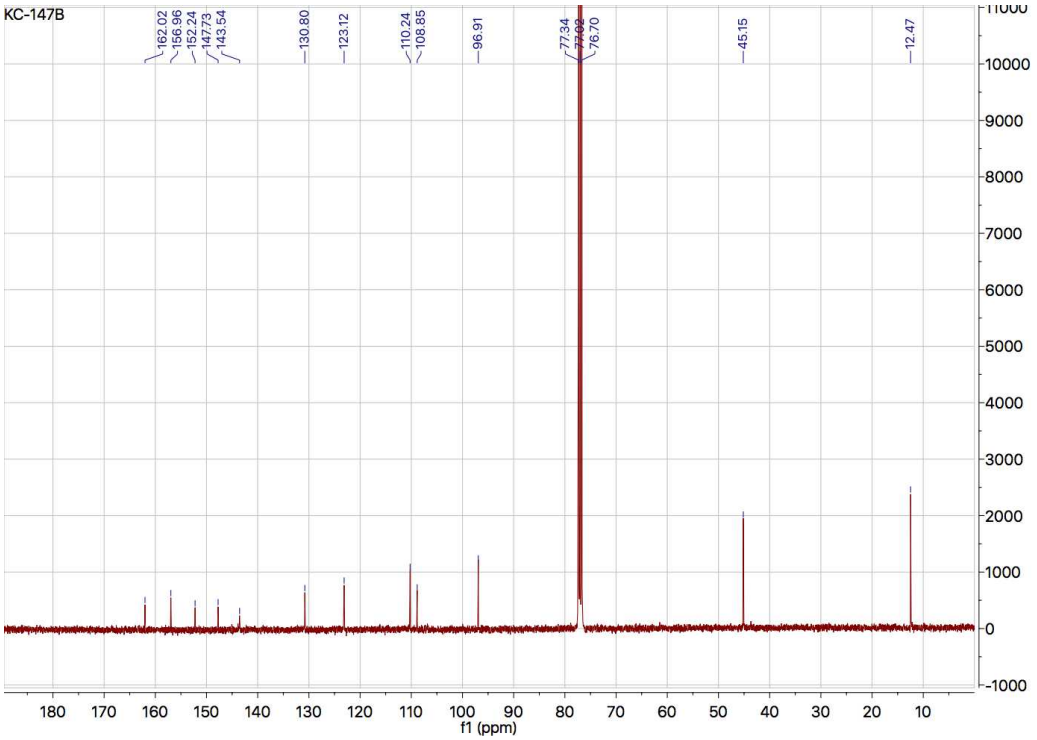

^{1}H & ^{13}C NMR of 10-(1*H*-benzo[d]imidazol-2-yl)-2,3,6,7-tetrahydro-1H-pyrano[2,3-f]pyrido[3,2,1-ij]quinolin-11(5H)-one (5b)

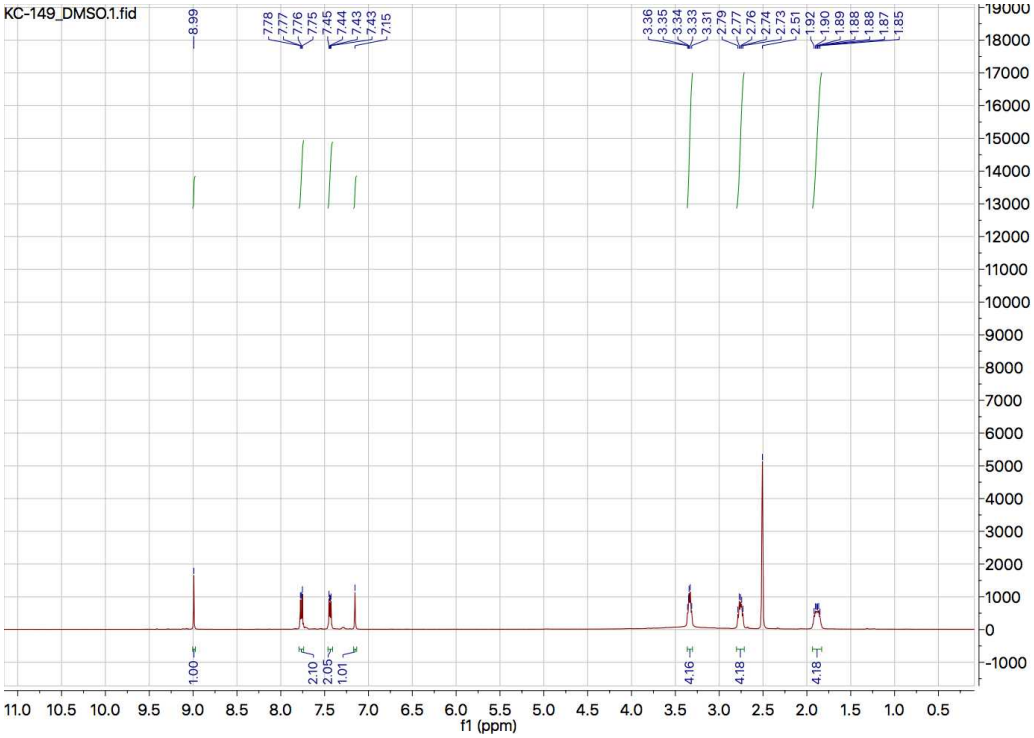

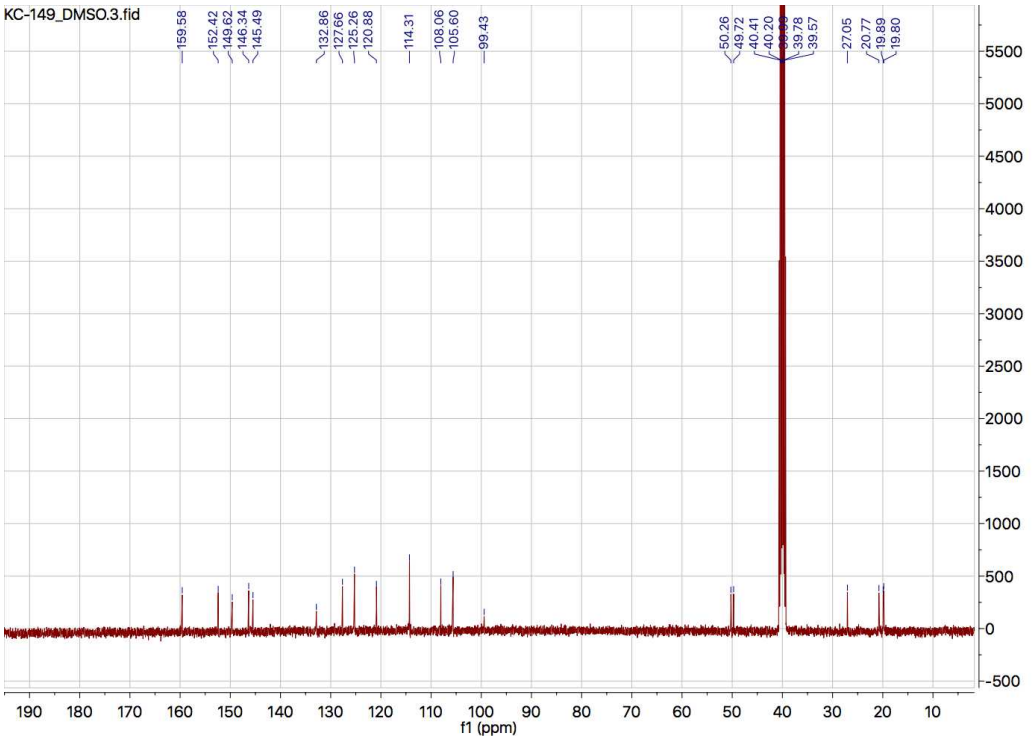

^{1}H & ^{13}C NMR of 2-(7-(diethylamino)-2-oxo-2H-chromen-3-yl)-3-methylbenzo[d]thiazol-3-ium iodide (**6a**)

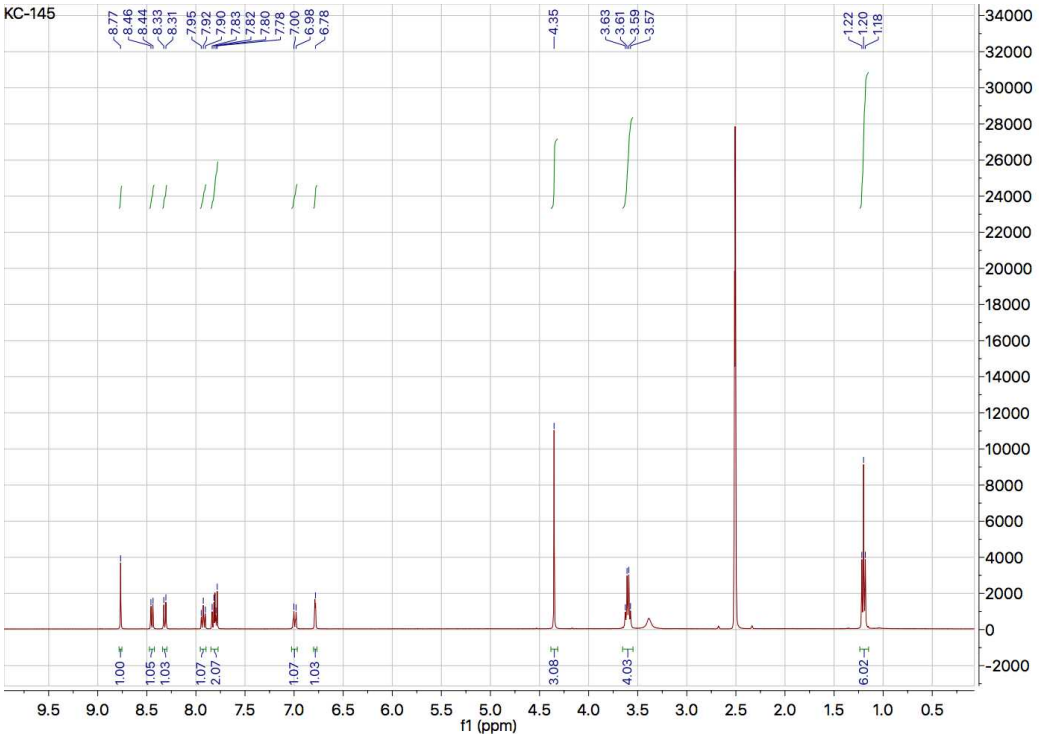

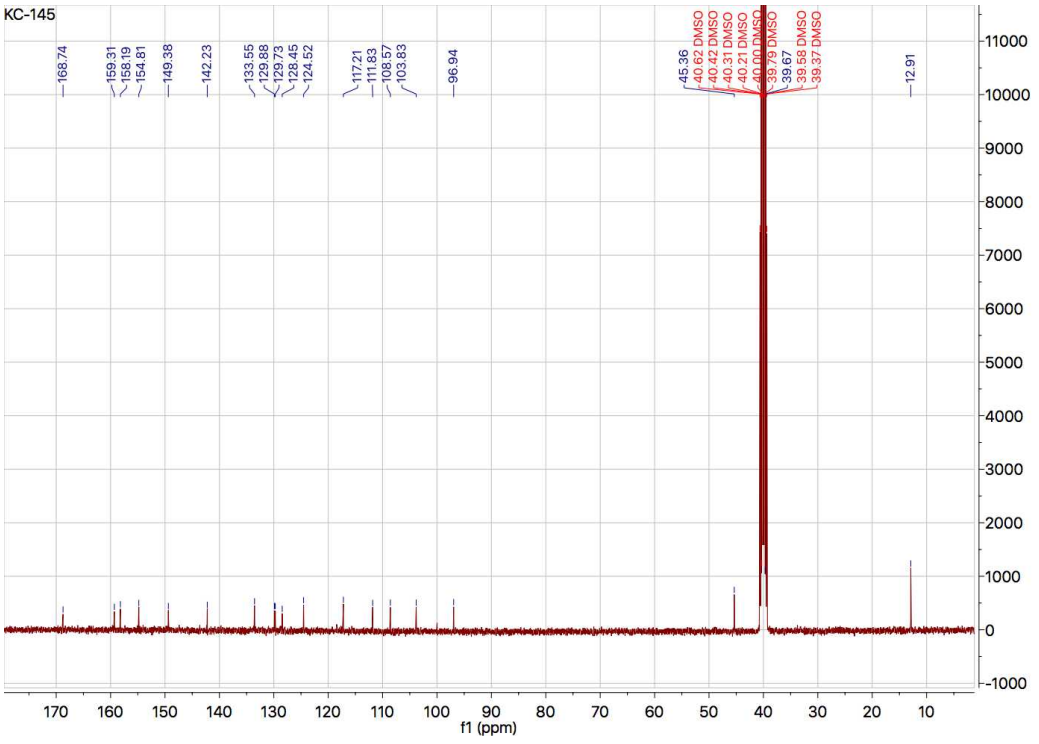

^{1}H & ^{13}C NMR of 3-methyl-2-(11-oxo-2,3,5,6,7,11-hexahydro-1*H*-pyrano[2,3-f]pyrido[3,2,1-ij]quinolin-10-yl)benzo[d]thiazol-3-ium iodide (**6b**)

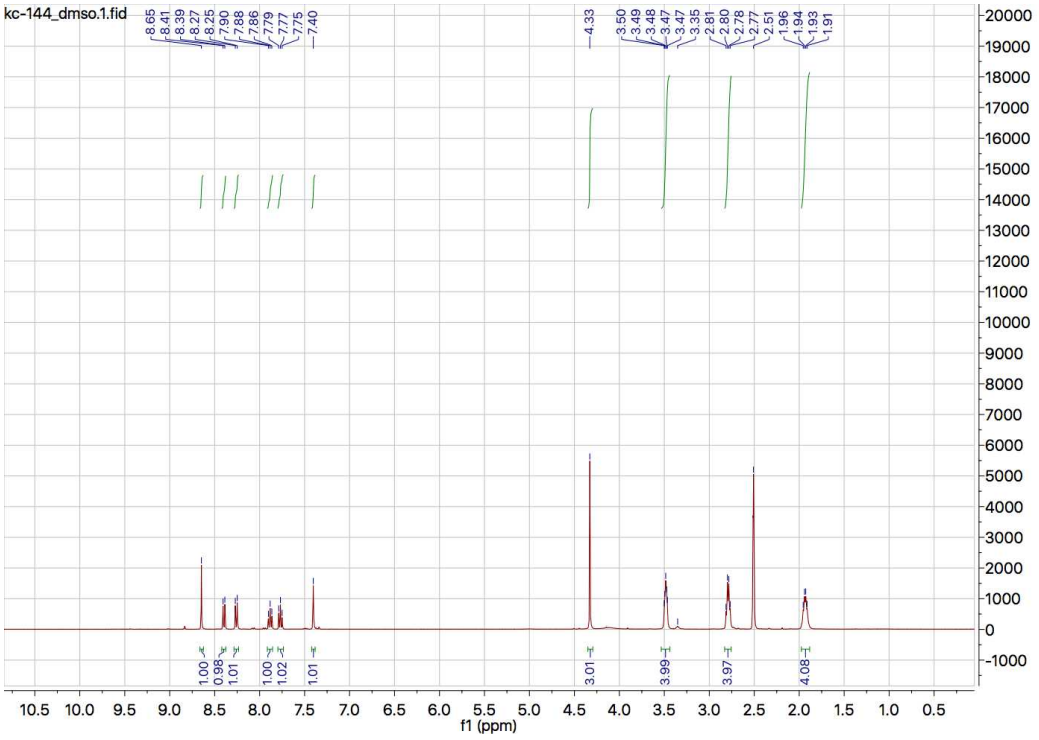

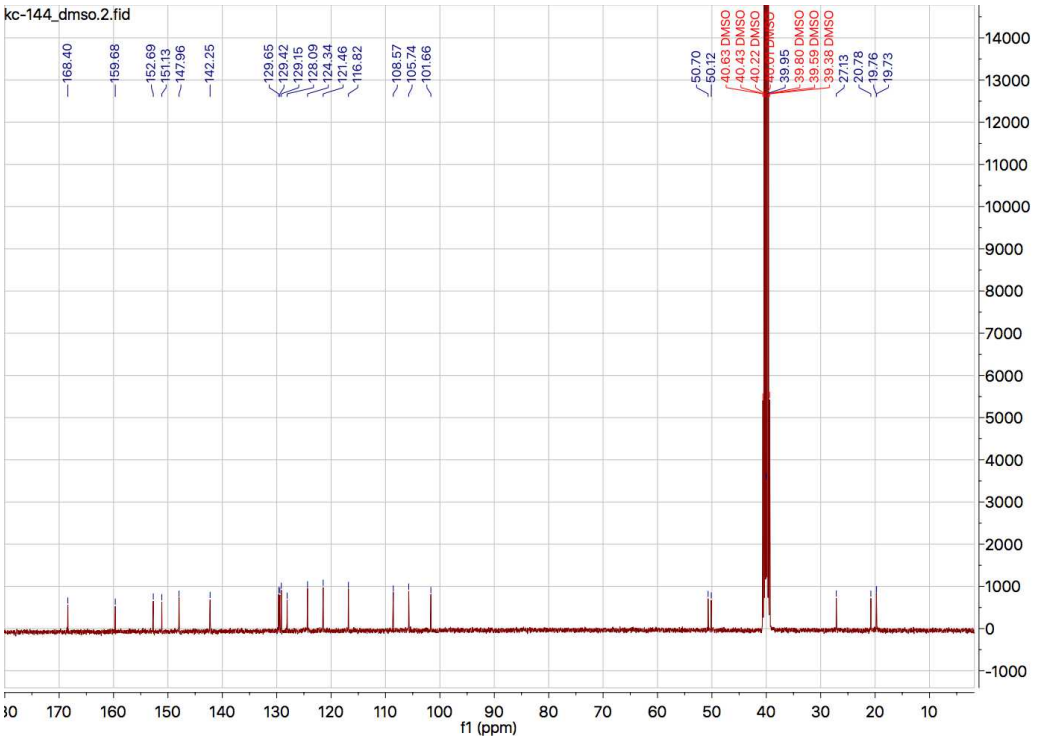

^{1}H & ^{13}C NMR of 2-(7-(diethylamino)-2-oxo-2H-chromen-3-yl)-1,3-dimethyl-1H-benzo[d]imidazol-3-ium iodide (6c)

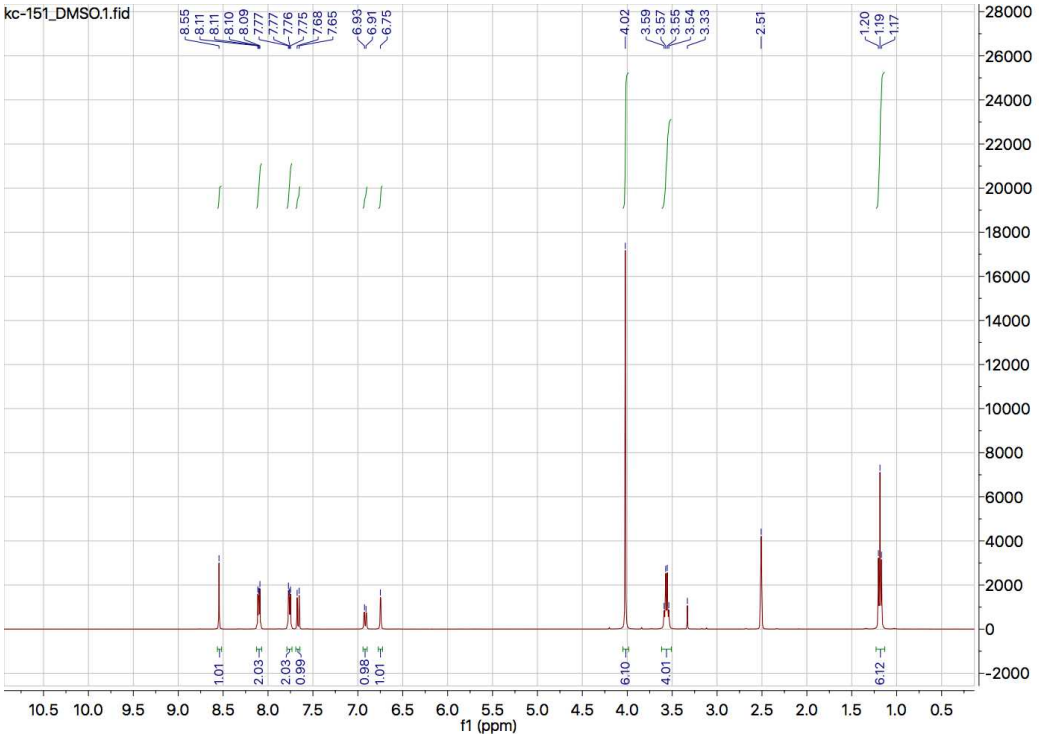

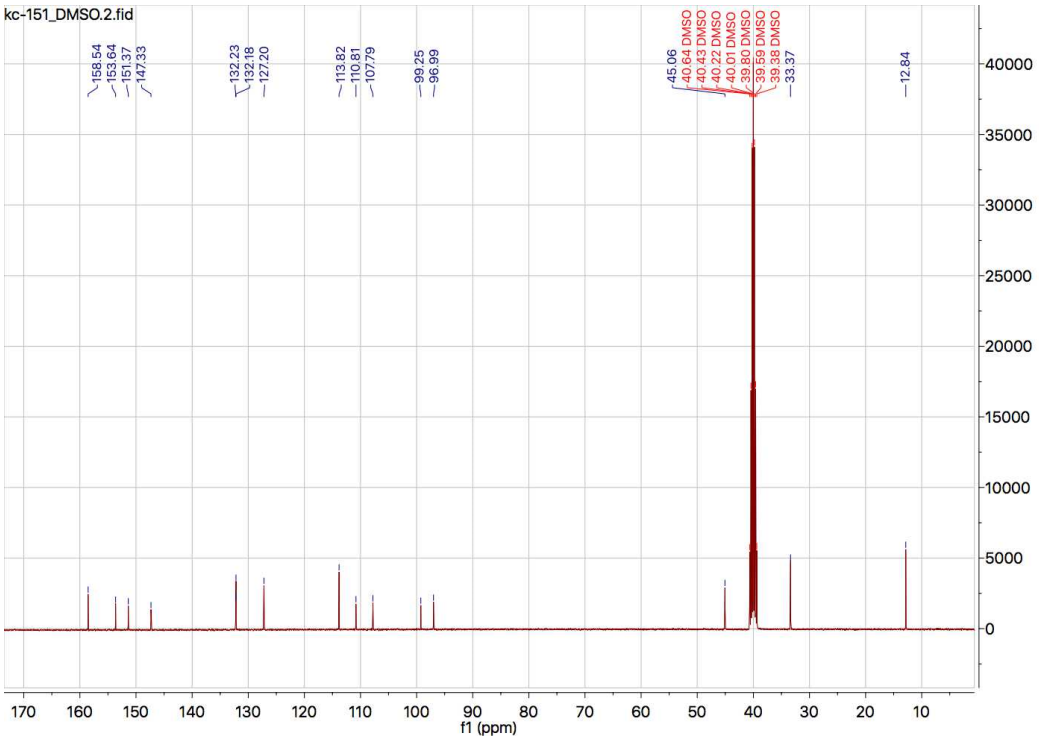

^{1}H & ^{13}C NMR of 1,3-dimethyl-2-(11-oxo-2,3,5,6,7,11-hexahydro-1H-pyrano[2,3-f]pyrido[3,2,1-ij]quinolin-10-yl)-1H-benzo[d]imidazol-3-ium iodide (6d)